Available online at www.sciencedirect.com
ScienceDirect
J. Chem. Thermodynamics 40 (2008) 335–352
JCT
www.elsevier.com/locate/jct

Review of uranyl mineral solubility measurements

Drew Gorman-Lewis *, Peter C. Burns, Jeremy B. Fein

University of Notre Dame, Department of Civil Engineering and Geological Sciences, 156 Fitzpatrick Hall, Notre Dame, IN 46556, United States

Received 19 September 2007; received in revised form 10 December 2007; accepted 12 December 2007
Available online 23 December 2007

Abstract

The solubility of uranyl minerals controls the transport and distribution of uranium in many oxidizing environments. Uranyl minerals form as secondary phases within uranium deposits, and they also represent important sinks for uranium and other radionuclides in nuclear waste repository settings and at sites of uranium groundwater contamination. Standard state Gibbs free energies of formation can be used to describe the solubility of uranyl minerals; therefore, models of the distribution and mobility of uranium in the environment require accurate determination of the Gibbs free energies of formation for a wide range of relevant uranyl minerals. Despite decades of study, the thermodynamic properties for many environmentally-important uranyl minerals are still not well constrained. In this review, we describe the necessary elements for rigorous solubility experiments that can be used to define Gibbs free energies of formation; we summarize published solubility data, point out difficulties in conducting uranyl mineral solubility experiments, and identify areas of future research necessary to construct an internally-consistent thermodynamic database for uranyl minerals.

Keywords: Uranium; Uranyl minerals; Solubility; Gibbs free energy; Thermodynamics

Contents

* Corresponding author. Present address: Department of Earth and Space Sciences, 4000 15th Avenue NE, Seattle, WA 98195-1310, USA.
E-mail address: dgormanl@u.washington.edu (D. Gorman-Lewis).

0021-9614/$ - see front matter © 2007 Elsevier Ltd. All rights reserved.
doi:10.1016/j.jct.2007.12.004

1. Introduction

Uranyl minerals form as secondary phases within U deposits, and also represent important sinks for U and other radionuclides in nuclear waste repository settings and at sites of U groundwater contamination [1]. The mobility and ultimate distribution of U in these environments is heavily impacted by the solubility of the important uranyl minerals present. Therefore, in order to understand the fate and transport of U in natural and contaminated settings, the solubilities and relative stabilities of uranyl minerals must be determined. Unfortunately, despite decades of study, the thermodynamic properties for many environmentally-important uranyl minerals are still not well constrained.

Exposure of UO_2 to oxygenated aqueous solutions favors the formation of uranyl oxide hydrates and uranyl silicates as secondary alteration products, with the exact paragenetic sequence dependent on the chemical composition of the system in question. Experiments on the alteration of spent nuclear fuel under simulated geologic repository conditions have identified uranyl oxide hydrates and uranyl silicates as important phases in the paragenetic sequence associated with the alteration. For example, Finch *et al.* [2] conducted unsaturated tests of alteration of spent nuclear fuel material in a laboratory setting, and examined the alteration products that formed over the course of 6 years. The groundwater that was used was from well J-13 at the Yucca Mountain site, and was reacted with crushed Tonopah Springs tuff at $T = 363$ K for 80 days prior to use (designated EJ-13 water). Significant alteration of the spent nuclear fuel occurred, and uranyl oxide hydrates and uranyl silicates were the main alteration products. Similarly, Wronkiewicz *et al.* [3,4] examined the alteration of un-irradiated UO_2, dripping EJ-13 water at $T = 363$ K onto the material for more than 10 years. Consistent with the observations of Finch *et al.* [2], uranyl oxide hydrates formed initially, and continued their alteration to uranyl silicates with continued exposure. Natural UO_2 deposits that have been oxidized, which can be good analogues to help understand the behavior of spent nuclear fuel in a geological repository, show a paragenetic sequence of alteration similar to that found in laboratory studies of spent nuclear fuel and UO_2 [5,6]. In addition to affecting U mobility in geologic repositories, uranyl minerals influence the mobility of U in a range of contaminated and natural settings [7–10].

Despite the potential importance of uranyl minerals affecting U mobility under oxidizing conditions, reliable solubility measurements of these phases, or thermodynamic properties upon which solubilities could be calculated, are lacking for many of these minerals. The results from a large number of solubility studies cannot be used to yield rigorously constrained thermodynamic data due to inappropriate experimental design or incomplete analyses (see discussion below). Recent reviews of the thermodynamic properties of U species [11,12] focus primarily on aqueous species, and contain few mineral solubility measurements. Mineral solubility measurements not only quantify the concentration of U and other mineral-forming cations that are in equilibrium with a particular mineral phase under specific aqueous conditions, but the results also can be used to calculate solubility product (K_{sp}) values and in turn the Gibbs free energy of formation for the mineral phase of interest. The Gibbs free energy of formation of a mineral enables the calculation of the solubility and relative stability of a mineral phase under conditions not directly studied in the laboratory, and represents a crucial parameter for predictions of repository performance and U mobility. In this paper, we review published solubility data for environmentally relevant uranyl phases; we compile the results, and we assess the quality of the measured parameters in order to identify the gaps in the current knowledge that need to be addressed in order to yield a useful internally-consistent thermodynamic database for the important uranyl phases. K_{sp} values for each mineral phase from each study considered here are compiled in table 1, which also explicitly shows the dissolution reaction and generalized mineral formula for each phase studied.

2. Mineral solubility measurements

Reliable measurements of the Gibbs free energy of formation of a mineral phase can be derived from solubility studies only when the following conditions are met: (1) the mineral of interest is demonstrated to be stable under the experimental conditions, (2) a true and demonstrable equilibrium state is attained during the experiments, and (3) the pH and aqueous metal concentrations present under the equilibrium conditions are measured. Thorough solid phase characterization is necessary for satisfying the first condition by identifying the mineral phase both before and after the solubility experiment using X-ray diffraction (XRD), spectroscopy approaches, and chemical analysis of the phase(s) present. Secondary phases or alteration products can easily precipitate during batch solubility experiments, and rigorous analyses are required to demonstrate the stability of the phase in question. The formation of secondary phases indicates that equilibrium with the original phase of interest was not attained, and therefore the thermodynamic properties for the original phase can not be determined from the experimental results unless both the primary and secondary phases are both in equilibrium with the aqueous phase. If equilibrium with both phases can be demonstrated, then it is still possible to obtain a rigorous value for K_{sp} by measuring the concentrations of all ions in solution and accounting for speciation of the ions. However, if the primary phase is altering to the secondary phase during the experiment, then it is not in equilibrium with the aqueous system and not possible to obtain a valid K_{sp} for the primary phase. XRD is essential in solubility experiments to identify the crystalline phase(s) present and to yield qualitative information on the degree of crystallinity of the phase(s); however, XRD does not detect

TABLE 1
Dissolution reactions

Mineral phase		$\lg K_{sp}$ ($I = 0$, unless noted)	Reference
	Uranyl carbonates		
Rutherfordine	$UO_2CO_3 = UO_2^{2+} + CO_3^{2-}$	−13.89 (± 0.11)[a]	[21]
	$UO_2CO_3 = UO_2^{2+} + CO_3^{2-}$	−14.91 (± 0.10)[b]	[22]
	$UO_2CO_3 = UO_2^{2+} + CO_3^{2-}$	−13.29 (± 0.01)[c]	[23]
Schröckingerite	$NaCa_3UO_2(CO_3)_3SO_4F(H_2O)_{10} = Na^+ + 3Ca^{2+} + UO_2^{2+} + 3CO_3^{2-} + SO_4^{2-} + F^- + 10H_2O$	−85.5 (± 1.5)[d]	[19]
Swartzite	$CaMgUO_2(CO_3)_3(H_2O)_{12} = Ca^{2+} + Mg^{2+} + UO_2^{2+} + 3CO_3^{2-} + 12H_2O$	−37.9 (± 1.4)[d]	[16]
Andersonite	$Na_2CaUO_2(CO_3)_3(H_2O)_6 = 2Na^+ + Ca^{2+} + UO_2^{2+} + 3CO_3^{2-} + 6H_2O$	−37.5 (± 4.2)[d]	[16]
Bayelite	$Mg_2UO_2(CO_3)_3(H_2O)_{18} = 2Mg^{2+} + UO_2^{2+} + 3CO_3^{2-} + 18H_2O$	−36.6 (± 1.4)[d]	[16]
Grimselite	$NaK_3UO_2(CO_3)_3(H_2O) = Na^+ + 3K^+ + UO_2^{2+} + 3CO_3^{2-} + H_2O$	−37.1 (± 0.3)[d]	[19]
Liebigite	$Ca_2UO_2(CO_3)_3(H_2O)_{10} = 2Ca^{2+} + UO_2^{2+} + 3CO_3^{2-} + 10H_2O$	−36.9 (± 2.1)[d]	[16]
	Uranyl oxide hydrates		
Metaschoepite	$2H^+ + UO_3(H_2O)_2 = UO_2^{2+} + 3H_2O$	5.52 (−0.04/+0.02)	[32]
	$2H^+ + UO_3(H_2O)_{2(amorphous)} = UO_2^{2+} + 3H_2O$	6.59 (± 0.14)[e]	[31]
	$2H^+ + UO_3(H_2O)_{2(crystalline)} = UO_2^{2+} + 3H_2O$	6.23 (± 0.14)[e]	[31]
	$2H^+ + UO_3(H_2O)_{2(amorphous)} = UO_2^{2+} + 3H_2O$	6.3 (± 0.1)	[33]
	$2H^+ + UO_3(H_2O)_{2(crystalline)} = UO_2^{2+} + 3H_2O$	5.9 (± 0.1)	[33]
	$2H^+ + UO_3(H_2O)_2 = UO_2^{2+} + 3H_2O$	5.14 (± 0.05)[f]	[22]
	$2H^+ + UO_3(H_2O)_2 = UO_2^{2+} + 3H_2O$	4.68 (± 0.14)[g]	[22]
	$2H^+ + UO_3(H_2O)_2 = UO_2^{2+} + 3H_2O$	5.72 (± 0.19) [h]	[21]
	$2H^+ + UO_3(H_2O)_2 = UO_2^{2+} + 3H_2O$	5.79 (± 0.19)[i]	[23]
Becquerelite	$14H^+ + Ca(UO_2)_6O_4(OH)_6(H_2O)_8 = Ca^{2+} + 6UO_2^{2+} + 18H_2O$	41.2 (± 0.52)	[35]
	$14H^+ + Ca(UO_2)_6O_4(OH)_6(H_2O)_8 = Ca^{2+} + 6UO_2^{2+} + 18H_2O$	43.2[j]	[39]
	$14H^+ + Ca(UO_2)_6O_4(OH)_6(H_2O)_8 = Ca^{2+} + 6UO_2^{2+} + 18H_2O$	29 (± 1)	[36]
	$14H^+ + Ca(UO_2)_6O_4(OH)_6(H_2O)_8 = Ca^{2+} + 6UO_2^{2+} + 18H_2O$	41.89 (± 0.52)[k]	[38]
	$14H^+ + Ca(UO_2)_6O_4(OH)_6(H_2O)_8 = Ca^{2+} + 6UO_2^{2+} + 18H_2O$	43.70 (± 0.47)	[38]
Compreignacite	$14H^+ + K_2(UO_2)_6O_4(OH)_6(H_2O)_7 = 2K^+ + 6UO_2^{2+} + 17H_2O$	36.82 (± 0.32)[l]	[38]
	$14H^+ + K_2(UO_2)_6O_4(OH)_6(H_2O)_7 = 2K^+ + 6UO_2^{2+} + 17H_2O$	39.16 (± 0.31)	[38]
Clarkeite-like	$3H^+ + Na(UO_2)O(OH) = Na^+ + UO_2^{2+} + 2H_2O$	8.81	[32]
	$3H^+ + Na(UO_2)O(OH) = Na^+ + UO_2^{2+} + 2H_2O$	9.02	[44]
	$3H^+ + Cs(UO_2)O(OH) = Cs^+ + UO_2^{2+} + 2H_2O$	8.61	[32]
$Cs(UO_2)O(OH)$	$3H^+ + Cs(UO_2)O(OH) = Cs^+ + UO_2^{2+} + 2H_2O$	9.27	[32]
	Uranyl silicates		
Soddyite	$4H^+ + (UO_2)_2SiO_4(H_2O)_2 = 2UO_2^{2+} + SiO_2 + 4H_2O$	6.43 (+0.20/ − 0.37)	[13]
	$4H^+ + (UO_2)_2SiO_4(H_2O)_2 = 2UO_2^{2+} + SiO_2 + 4H_2O$	5.74 (± 0.21)	[45]
	$4H^+ + (UO_2)_2SiO_4(H_2O)_2 = 2UO_2^{2+} + SiO_2 + 4H_2O$	6.03 (± 0.45)[m]	[50]
	$4H^+ + (UO_2)_2SiO_4(H_2O)_2 = 2UO_2^{2+} + SiO_2 + 4H_2O$	6.15 (± 0.53)	[50]
Sodium boltwoodite	$3H^+ + Na[UO_2(SiO_3OH)](H_2O)_{1.5} = UO_2^{2+} + Na^+ + H_4SiO_4 + 1.5H_2O$	5.86 (± 0.24)	[47]
	$3H^+ + Na[UO_2(SiO_3OH)](H_2O)_{1.5} = UO_2^{2+} + Na^+ + H_4SiO_4 + 1.5H_2O$	5.85 (± 0.26)	[47]
	$3H^+ + NaH_3O(UO_2)SiO_4H_2O = UO_2^{2+} + Na^+ + SiO_2 + 4H_2O$	5.82 (± 0.16)	[45]
Uranophane	$6H^+ + Ca(H_3O)_2(UO_2)_2(SiO_4)_2(H_2O)_3 = Ca^{2+} + 2UO_2^{2+} + 2SiO_2 + 9H_2O$	9.42 (± 0.48)	[45]
	$6H^+ + Ca(H_3O)_2(UO_2)_2(SiO_4)_2(H_2O)_3 = Ca^{2+} + 2UO_2^{2+} + 2SiO_2 + 9H_2O$	6.5[n]	[48]
	$6H^+ + Ca(H_3O)_2(UO_2)_2(SiO_4)_2(H_2O)_3 = Ca^{2+} + 2UO_2^{2+} + 2SiO_2 + 9H_2O$	7.8 (±0.8)[o]	[48]
Sodium weeksite	$6H^+ + Na_2(UO_2)_2(Si_2O_5)_3(H_2O)_4 = 2Na^+ + 2UO_2^{2+} + 6SiO_2 + 7H_2O$	1.50 (± 0.08)	[45]
	Uranyl phosphates		
Chernikovite	$H_3O(UO_2)PO_4(H_2O)_3 = H_3O^+ + UO_2^{2+} + PO_4^{3-} + 3H_2O$	−22.73 (± 0.24)[p]	[61]
Meta-ankoleite	$KUO_2PO_4(H_2O)_4 = K^+ + UO_2^{2+} + PO_4^{3-} + 4H_2O$	−24.30 (± 0.81)[p]	[61]
Uranyl hydrogen phosphate	$UO_2HPO_4(H_2O)_4 = UO_2^{2+} + HPO_4^{2-} + 4H_2O$	−12.17 (± 0.07)	[56]
	$UO_2HPO_4(H_2O)_4 = UO_2^{2+} + HPO_4^{2-} + 4H_2O$	−12.33 (± 0.06)	[57]
Uranyl orthophosphate	$(UO_2)_3(PO_4)_2(H_2O)_4 = 3UO_2^{2+} + 2PO_4^{3-} + 4H_2O$	−49.7 (± 0.3)	[56]
	$(UO_2)_3(PO_4)_2(H_2O)_4 = 3UO_2^{2+} + 2PO_4^{3-} + 4H_2O$	−53.33 (± 0.17)	[31]
	$(UO_2)_3(PO_4)_2(H_2O)_4 = 3UO_2^{2+} + 2PO_4^{3-} + 4H_2O$	−49.00 (± 0.80)	[57]
	$(UO_2)_3(PO_4)_2(H_2O)_4 = 3UO_2^{2+} + 2PO_4^{3-} + 4H_2O$	−49.08 (± 0.48)	[59]
$MUO_2PO_4(H_2O)_x$	$NH_4UO_2PO_4(H_2O)_3 = NH_4^+ + UO_2^{2+} + PO_4^{3-} + 3H_2O$	−26.50 (± 0.09)	[58]
	$NH_4UO_2PO_4(H_2O)_x = NH_4^+ + UO_2^{2+} + PO_4^{3-} + xH_2O$	−26.23 (± 0.20)	[56]
	$KUO_2PO_4(H_2O)_3 = K^+ + UO_2^{2+} + PO_4^{3-} + 3H_2O$	−26.28 (± 0.25)	[60]
	$KUO_2PO_4(H_2O)_x = K^+ + UO_2^{2+} + PO_4^{3-} + xH_2O$	−25.50 (± 0.10)[q]	[56]
	$NaUO_2PO_4(H_2O)_x = Na^+ + UO_2^{2+} + PO_4^{3-} + xH_2O$	−24.21 (± 0.07)[q]	[56]
	$RbUO_2PO_4(H_2O)_x = Rb^+ + UO_2^{2+} + PO_4^{3-} + xH_2O$	−25.72 (± 0.15)[q]	[56]
	$CsUO_2PO_4(H_2O)_x = Cs^+ + UO_2^{2+} + PO_4^{3-} + xH_2O$	−25.41 (± 0.20)[q]	[56]
	Uranyl peroxides		
Metastudtite	$UO_4(H_2O)_2 = UO_2^{2+} + O_2^{2-} + 2H_2O$	−35.88 (± 0.01)[r]	[66]
Studtite	$UO_2O_2(H_2O)_4 + 2H^+ = UO_2^{2+} + H_2O_2 + 4H_2O$	−2.88 to −2.86[s]	[62]

(*continued on next page*)

TABLE 1 (*continued*)

Mineral phase		$\lg K_{sp}$ ($I = 0$, unless noted)	Reference
	Uranyl sulfates		
Zippeite	$Mg_2(UO_2)_6(SO_4)_3(OH)_{10}(H_2O)_x = 2Mg^{2+} + 6UO_2^{2+} + 3SO_4^{2-} + 10OH^- + xH_2O$	−146.1	[69]
	$Co_2(UO_2)_6(SO_4)_3(OH)_{10}(H_2O)_x = 2Co^{2+} + 6UO_2^{2+} + 3SO_4^{2-} + 10OH^- + xH_2O$	−145.9	[69]
	$Ni_2(UO_2)_6(SO_4)_3(OH)_{10}(H_2O)_x = 2Ni^{2+} + 6UO_2^{2+} + 3SO_4^{2-} + 10OH^- + xH_2O$	−145.6	[69]
	$Zn_2(UO_2)_6(SO_4)_3(OH)_{10}(H_2O)_x = 2Zn^{2+} + 6UO_2^{2+} + 3SO_4^{2-} + 10OH^- + xH_2O$	−153.0	[69]
	$Na_4(UO_2)_6(SO_4)_3(OH)_{10}(H_2O)_4 = 4Na^+ + 6UO_2^{2+} + 3SO_4^{2-} + 10OH^- + 4H_2O$	−116.5[t]	[70]
	$K_4(UO_2)_6(SO_4)_3(OH)_{10}(H_2O)_4 = 4K^+ + 6UO_2^{2+} + 3SO_4^{2-} + 10OH^- + 4H_2O$	−116.1[t]	[70]
	$(NH_4)_4(UO_2)_6(SO_4)_3(OH)_{10}(H_2O)_4 = 4NH_4^+ + 6UO_2^{2+} + 3SO_4^{2-} + 10OH^- + 4H_2O$	−126.2[t]	[70]

[a] Ionic strength 0.1 M; not corrected to infinite dilution value. Data obtained under 100% CO_2.
[b] Data obtained under 100% CO_2.
[c] Ionic strength 0.1 M; not corrected to infinite dilution value.
[d] K_{sp} calculated from reported standard state Gibbs free energy of formation.
[e] Values recalculated from [33].
[f] Data obtained under 0.03% CO_2.
[g] Data obtained under 0.3% CO_2.
[h] Data obtained under 0.03 and 0.98% CO_2; ionic strength 0.1 M; not corrected to infinite dilution value.
[i] Ionic strength 0.1 M; not corrected to infinite dilution value.
[j] Ionic strength not specified and no apparent extrapolation to I = 0.
[k] Calculated from the alteration of metaschoepite.
[l] Calculated from the alteration of metaschoepite.
[m] Value from experiments performed under an atmosphere of N_2.
[n] K_{sp} calculated based on solution concentrations not activities. See text for details.
[o] K_{sp} calculated from solution concentrations not activities, ionic strength not reported.
[p] Ionic strength 0.2 M; not corrected to infinite dilution value.
[q] K_{sp} calculated based on solution concentrations not activities. See text for details.
[r] Ionic strength 0.7 M; not corrected to infinite dilution value.
[s] Ionic strength not specified; not corrected to infinite dilution value.
[t] K_{sp} calculated from reported standard state Gibbs free energy of formation.

phases if they represent less than approximately 4% to 5% of the total solids or if they are amorphous. Fourier transform infrared spectroscopy (FTIR) is a complementary technique to XRD in that it allows for the identification of the presence of amorphous materials that may have precipitated during the course of the solubility experiment.

Attainment of mineral-water chemical equilibrium can only be demonstrated via reversibility experiments; that is, approaching the equilibrium state from supersaturated as well as from undersaturated conditions with respect to the dissolved elements of interest. Reaching a concentration plateau, or steady state, is not a sufficient condition to demonstrate chemical equilibrium in an experimental system. pH and aqueous metal concentration measurements are crucial in order to calculate the ionic strength of the experimental solution and, hence, the activity coefficients (and activities) of aqueous species in the solution. When calculating uranyl activity, it is necessary to consider complexation of uranyl by hydroxide and carbonate. In solutions under low pH conditions and low U concentrations (below *ca.* pH 4 and 10 mM) it is reasonable to assume that all of the measured U in solution is present in the form of the uncomplexed uranyl cation. However, experiments performed above pH 4 or with high concentrations of U or complexing ligands may have a significant concentration of complexed uranyl ion. The complex speciation of uranyl at high pH produces a number of highly charged species in solution and can lead to inaccurate activity calculations due to magnified uncertainties in activity coefficients for these aqueous species. Typically, geochemical codes calculate aqueous speciation through an iterative approach that starts from a first approximation input by the user. Techniques such as limiting initial calculations to the dominant species and subsequently adding minor species into the calculation after the initial convergence can improve the first approximation to promote successful calculations. In general, all aqueous complexation for each ion in solution must be accounted for; hence, stability constants for aqueous complexes must be known for the system of interest.

Measurements of the concentrations of ions in solution can be used to calculate the K_{sp} of the solid phase of interest, and thereby to calculate the Gibbs free energy of formation of the phase. For example, the dissolution reaction of soddyite ($(UO_2)SiO_4(H_2O)_2$) can be represented as follows:

$$4H^+ + (UO_2)_2SiO_4(H_2O)_2 = 2UO_2{}^{2+} + SiO_2 + 4H_2O \quad (1)$$

For aqueous species, $a = m \cdot \gamma$, where a represents aqueous activity of a species, m represents the molality of the species, and γ is the activity coefficient of the species. A number of equations have been proposed in order to calculate activity coefficients (see below), and thus it is important

to specify the equation type and the equation parameter values that are used in these calculations. Also, any use of an activity coefficient requires a strict definition of standard state for the species in question, and for this example the standard states for solid phases and for H_2O are defined as the pure mineral and fluid, respectively, at the pressure and temperature of interest. The standard state for aqueous species is defined as a hypothetical one molal solution whose behavior is that of infinite H_2O dilution at the pressure and temperature of interest. Molal activity coefficients for neutral aqueous species are assumed to be unity. Like Gorman-Lewis *et al.* [13], we calculate activity coefficients using the extended Debye–Hückel Equation (2):

$$\lg \gamma_i = \frac{-Az_i^2\sqrt{I}}{1 + aB\sqrt{I}} + bI, \tag{2}$$

where I and z_i represent the ionic strength and ionic charge, respectively; A and B are constants at a given temperature and pressure, with values of 0.5105 and 0.3285, respectively, under ambient conditions; and a and b are electrolyte-specific constants [14].

Given these standard state definitions, and assuming that the solid phase in question is pure and that the activity of water is unity for this example, the K_{sp} for soddyite can be expressed as

$$K_{sp} = \frac{a^2_{UO_2^{2+}} \times a_{SiO_{2(aq)}}}{a^4_{H^+}}. \tag{3}$$

The K_{sp} value can be used to calculate the change in the standard state molal Gibbs free energy associated with the dissolution reaction (ΔG°_{rxn}):

$$\Delta G^\circ_{rxn} = -2.303RT \cdot \lg K_{sp}, \tag{4}$$

where R is the universal gas constant and T is absolute temperature. The ultimate thermodynamic goal for solubility experiments, however, is to determine the standard state Gibbs free energy of formation of the mineral phase of interest (ΔG°_f), and this can be accomplished if the standard state Gibbs free energies of formation for the other species in the dissolution reaction are known. For the soddyite case:

$$\Delta G^\circ_{f(soddyite)} = 2 \times \Delta G^\circ_{f(UO_2^{2+})} + \Delta G^\circ_{f(SiO_{2(aq)})} + 4 \times \Delta G^\circ_{f(H_2O)} - \Delta G^\circ_{rxn} \tag{5}$$

Rigorous and internally-consistent constraints on the values of the standard state Gibbs free energies of formation for uranyl mineral phases can be used for two important applications: (1) the values can be used to determine the relative stabilities of the large number of possible uranyl mineral phases that may form as a function of aqueous solution composition, pressure, and temperature and (2) the thermodynamic properties can be used to calculate the aqueous cation concentrations that are in equilibrium with each potential phase of environmental or geologic interest for any given condition of interest.

3. Previous studies

3.1. Uranyl carbonates

The uranyl tricarbonate species is extremely stable and soluble in aqueous solutions; however, should these solutions become concentrated, *i.e.* due to evaporation, a range of uranyl carbonate minerals can form, the specific identity of which is a function primarily of the concentration of other ions in solution [15]. These mineral phases may not be dominant in repository settings but are commonly found in mining environments as the oxidized products of U ore [16]. The extreme solubility of these minerals, as compared to uranyl oxide hydrates and uranyl silicates, can make them act as transitional phases in the alteration that can occur as uraninite oxidizes and U becomes soluble [16].

Alwan and Williams [16] reported standard state Gibbs free energy of formation values for liebigite ($Ca_2UO_2(CO_3)_3(H_2O)_{10}$), swartzite ($CaMgUO_2(CO_3)_3(H_2O)_{12}$), bayleyite ($Mg_2UO_2(CO_3)_3(H_2O)_{18}$), and andersonite ($Na_2K_3UO_3(CO_3)_3(H_2O)_6$) based on solubility experiments at five different temperatures under a CO_2-free atmosphere. After one week, the experimental solutions were sampled and analyzed for U only. The authors assumed stoichiometric dissolution of the mineral phases and calculated the sodium, calcium, and magnesium concentrations based on the measured U concentration of each sample. Using a modified Davies equation with parameters from Truesdell and Jones [17] and Kielland [18], the authors calculated uranyl activities from total dissolved U measurements while accounting for aqueous uranyl complexation. It is unclear whether the authors checked the final mineral residue to verify whether the phases were stable under the experimental conditions and that mineral dissolution was indeed stoichiometric. The $\lg K_{sp}$ values calculated from their reported Gibbs free energy of formation for liebigite, swartzite, bayelite, and andersonite are (-36.9 ± 2.1), (-37.9 ± 1.4), (-36.6 ± 1.4), and (-37.5 ± 4.2), respectively.

O'Brien and Williams [19] reported standard state Gibbs free energies of formation for grimselite ($NaK_3UO_2(CO_3)_3H_2O$) and schröckingerite ($NaCa_3UO_2(CO_3)_3SO_4F(H_2O)_{10}$) based on solubility measurements. The synthesis for schröckingerite involved using gypsum as a starting material, and consequently ended up with gypsum as an impurity in schröckingerite. Solubility experiments were carried out from pH 7.7 to 8.5 and at $T = 293.2$ K and $T = 298.2$ K; however, K_{sp} calculations were based on data from $T = 298.2$ K only. U and SO_4^{2-} were the only species measured in the schröckingerite experiments. Even though there were no measurements of sodium and calcium concentrations in solution, schröckingerite dissolution was assumed to be stoichiometric. By measuring the U concentration in solution, the authors calculated the uranyl activity using a modified Davies equation with parameters from Truesdell and Jones [17] and Kielland [18] and taking into account various uranyl hydroxide and uranyl carbonate

complexes. The authors stated that they used XRD analysis of the final mineral residue in the schröckingerite systems to determine congruent dissolution; however, there is no mention of the degree of crystallinity of the mineral residue, *i.e.* if there was any decrease in crystallinity. Grimselite solubility was calculated in a similar manner to schröckingerite in that only dissolved U was analyzed in each sample, and sodium and potassium concentrations were calculated assuming stoichiometric dissolution. However, the authors do not mention any checks of the final mineral residue in the grimselite experiments for possible alteration. The $\lg K_{sp}$ values for schröckingerite and grimselite calculated from the reported Gibbs free energy of formation are (-85.5 ± 1.5) and (-37.1 ± 0.3), respectively.

The assumption of stoichiometric dissolution is a substantial weakness in these studies. XRD analysis cannot conclusively determine stoichiometric dissolution. Leaching of cations from the surface of the mineral in contact with the aqueous phase is possible, and protons can replace the leached ions to maintain charge balance [20]. The resulting XRD pattern would only indicate some loss in crystallinity, and only if this leached layer were quite extensive. The only way to convincingly determine stoichiometric dissolution is by measuring all the ions in solution. Neither the O'Brien and Williams study nor the Alwan and Williams study explicitly stated that the solid phases used in each experiment had not altered, with the exception of the verification of schröckingerite. Mineral residue verification is essential for demonstrating mineral phase stability under the experimental conditions.

The measured solubilities for rutherfordine (UO_2CO_3) vary considerably. Rutherfordine is a uranyl carbonate composed of uranyl hexagonal bipyramid sheets held together through van der waals forces, and is the least soluble of the uranyl carbonates. Meinrath and Kimura [21] precipitated rutherfordine from a 0.002 M uranyl solution from pH 2.8 to 4.6 under 100% CO_2 with the system left to equilibrate for 3 weeks. Pre-experimental solid phase characterization by DTA (differential thermal analysis), TGA (thermogravimetric analysis), FTIR, solid phase UV–Vis spectroscopy (ultraviolet and visible spectroscopy), and XRD verified the mineral phase; however, there is no explicit mention of post-experimental characterization. Using pH titrations with the mineral suspended in a 0.1 M $NaClO_4$ solution to buffer ionic strength, additions of 0.1 M $HClO_4$ and 0.05 M Na_2CO_3 were added to the suspension to obtain solubility data from super saturated and undersaturated conditions. The authors state that a steady state was reached in 2–3 days; however, there was no mention of how they determined the steady-state conditions, *i.e.* pH stability or multiple U analyses at the same titration point. The resulting $\lg K_{sp}$ was (-13.89 ± 0.11) which did take into account aqueous complexation of uranyl. However, the authors did not make corrections for ionic strength and consequently their value is only valid at 0.1 M ionic strength. Meinrath *et al.* [22] used similar techniques as the previous study but conducted the experiments under a 8% CO_2 atmosphere. In this study, the authors explicitly stated that the solid phases were characterized continuously throughout the titrations; however, there was no mention of equilibration times or how steady states were determined. To calculate activities, the authors used single ion activity coefficients of $10^{-0.40}$, $10^{-0.46}$, and $10^{-0.09}$ for UO_2^{2+}, CO_3^{2-}, and H^+, respectively. There is no comment on the origin of the activity coefficient values. Taking into account aqueous uranyl complexation the authors determined a $\lg K_{sp}$ of (-14.91 ± 0.10).

Another study that reports rutherfordine solubility measurements, performed by Kramer-Schnabel *et al.* [23], conducted experiments from undersaturated conditions in an open system with CO_2 equilibrated with the atmosphere and in a closed system at constant CO_2 partial pressure. Characterization of pre- and post-experimental mineral phases by XRD confirmed the starting mineral as rutherfordine and that it was stable under the experimental conditions. The difficulty in determining the total carbonate in solution and the small losses of CO_2 during the closed system experiments caused the authors to only use the open system data for their K_{sp} calculations which produced a $\lg K_{sp}$ of (-13.29 ± 0.01). While their $\lg K_{sp}$ calculations did account for aqueous complexation of uranyl, the calculations were done using aqueous concentrations and not activities, making their value only valid at an ionic strength of 0.1 M.

The discrepancy of the K_{sp} values produced by Meinrath and Kimura [21] and Kramer-Schnabel [23] under an open atmosphere highlights the difficulty in obtaining consistent results. Meinrath *et al.* [22] did characterize their mineral phase more thoroughly and obtained better-constrained data by measuring the solubility from supersaturated conditions as well as undersaturated conditions. Some of the discrepancy may arise because measuring the solubility of uranyl carbonates is particularly difficult due to their high solubility and difficulties associated with attempting to control atmospheric compositions. More rigorous measurements of the solubilities of the various uranyl carbonate solid phases are necessary. Under naturally occurring conditions, these phases may be most important as intermediary phases, and it is possible that they can affect U mobility in groundwater settings.

3.2. Uranyl oxide hydrates

Uranyl oxide hydrates are usually the first alteration products to appear where uraninite is oxidized in U deposits [1]. Experiments performed to gain a better understanding of the paragenetic sequence of alteration products of spent nuclear fuel under simulated Yucca Mountain conditions identified uranyl oxide hydrates, such as becquerelite, compreignacite, metaschoepite, and schoepite, as the first alteration phases formed [3,4]. Schoepite and metaschoepite may be important surfaces for the adsorption of actinides such as Np, while becquerelite could possibly sequester Sr through incorporation into its mineral structure [24].

Burns *et al.* [25] predicted that incorporation of transuranic elements into uranyl oxide hydrates could significantly impact their future mobility under repository conditions. Recent studies have indicated that Np^{5+} can be incorporated into some uranyl oxide hydrates [26–28].

Schoepite ($(UO_3(H_2O)_{2.25})$ and $([(UO_2)_8O_2(OH)_{12}](H_2O)_{12}$) chemical and structural formulas, respectively) and metaschoepite ($(UO_3(H_2O)_2)$ and $([(UO_2)_4O(OH)_6](H_2O)_5$) chemical and structural formulas, respectively) are uranyl oxide hydrates that possess electroneutral sheets of uranyl pentagonal bipyramids, with no interlayer cations. The hydration states of the two phases differ by 0.25 waters [29]. Although the two phases have distinct crystal structures [30], they are often erroneously treated as equivalent phases in the literature. In our discussion of previous studies, $UO_3 \cdot 2H_2O$ will be referred to as metaschoepite and $UO_3 \cdot 2.25H_2O$ will be referred to as schoepite. In contrast to the situation for many uranyl minerals, the solubility of metaschoepite has been measured by a number of researchers. The $\lg K_{sp}$ from the literature range from (4.68) to (6.23) [21,31]. The following studies provide either direct or indirect constraints on the solubility of metaschoepite.

Giammar *et al.* [32] measured the solubility of metaschoepite as a part of a study aimed at determining the influence of dissolved sodium and cesium concentrations on uranyl oxide hydrate solubility. The authors performed batch experiments by adding metaschoepite to solutions of $NaNO_3$, $CsNO_3$, or NaF, and by equilibrating metaschoepite with water for 43 days before adding concentrated aliquots of $NaNO_3$, $CsNO_3$, or NaF. Metaschoepite that was equilibrated with water prior to the addition of concentrated Na or Cs solutions did not form new mineral phases by incorporating of Na or Cs; however, new phases that incorporated Na and Cs did form in experiments where metaschoepite initially equilibrated with solutions already containing Na or Cs. A clarkeite-like ($Na(UO_2)O(OH)$) phase was formed in the sodium-bearing experiments, and a cesium uranyl oxide hydrate ($Cs(UO_2)O(OH)$), not previously described, formed in the cesium-bearing experiments. Mineral residues from the experiments were characterized by XRD, Raman spectroscopy, and scanning electron microscopy. Using the Davies equation, the authors calculated uranyl activities taking into account aqueous complexation of uranyl ions. Solubility measurements of metaschoepite from undersaturated conditions for experiments in which no new mineral phases were formed yielded a $\lg K_{sp}$ of $(5.52\ -0.04/+0.02)$. Estimated $\lg K_{sp}$ values for the clarkeite-like and Cs uranyl oxide hydrate were possible from experiments where mineral residues showed complete alteration to the new phase. The clarkeite-like phase produced $\lg K_{sp}$ values of (8.81) and (8.61) determined from two experimental runs, and the Cs uranyl oxide hydrate experiment yielded a $\lg K_{sp}$ of (9.27).

Bruno and Sandino [33] measured the solubility of metaschoepite and an amorphous uranyl oxide hydrate ($(UO_3(H_2O)_2)$). Syntheses involved precipitation from a $UO_2(ClO_4)_2$ solution with NaOH added dropwise under a constant stream of N_2. The characterization of the precipitate by XRD immediately following the synthesis indicated that the material was likely an amorphous uranyl oxide hydrate of similar composition to metaschoepite. After the material was left for a few weeks under a stream of N_2 to crystallize at room temperature, a fine-grained yellow phase formed which was crystalline metaschoepite. From undersaturated conditions, the authors performed solubility measurements of both the amorphous and crystalline phases from pH 6.8 to 9.0. Using the specific ion interaction (SIT) theory with the Brønsted–Guggenheim–Scathard (BGS) [11] approach the authors calculated uranyl ion activities taking into account aqueous complexation of the uranyl ion. The data yielded $\lg K_{sp}$ values of (5.9 ± 0.1) and (6.3 ± 0.1) for the crystalline and amorphous phases, respectively. A recalculation of the K_{sp} values in a subsequent study by Sandino and Bruno [31], using the same approach as the previous study to calculate uranyl activities, produced $\lg K_{sp}$ values of (6.23 ± 0.14) and (6.59 ± 0.14) for crystalline and amorphous phases, respectively. While all K_{sp} values took into account aqueous uranyl complexation, the recalculated values used a newly calculated stability constant for an aqueous uranyl hydroxide species.

Kramer-Schnabel *et al.* [23] measured the solubility of metaschoepite from supersaturation in 0.1 M $NaClO_4$. The authors gathered data from pH 4.36 to 5.71 by adjusting the pH of uranyl nitrate solutions with sodium hydroxide and allowing the subsequent precipitate to reach equilibrium (3 to 14 days). Separating the resulting precipitates from solution, the authors dried and characterized the precipitates by XRD to confirm the identity of the solid phase as metaschoepite. Although metaschoepite was stable from pH 4.5 to 5.5, above pH 5.5, the resulting solid phase was uranyl diuranate (formula not specified). While the authors did account for aqueous complexation of the uranyl ion by hydroxide and carbonate in their K_{sp} calculations, they did not calculate activities of the aqueous species; therefore, the calculated $\lg K_{sp}$ value of (5.79 ± 0.19) is a conditional constant, only valid at an ionic strength of 0.1 M.

Meinrath and Kimura [21] precipitated solids from a 2 mM uranyl solution (the anion of the uranyl salt is not mentioned) with the addition of 0.05 M Na_2CO_3 under atmospheres of pure CO_2, 0.98% CO_2, and 0.03% CO_2. The precipitated systems were left to equilibrate for 3 weeks. Identification of the precipitates by continuous characterization throughout the experiments with DTA, TGA, FTIR, solid phase UV–Vis spectroscopy, and XRD revealed rutherfordine in the pure CO_2 system and metaschoepite in the other atmospheric compositions. Rutherfordine solubility data is discussed above. To gather solubility data for metaschoepite, the authors performed titrations of the equilibrated experimental systems from pH 2.8 to 4.6 with the addition of 0.1 M NaOH to obtain solubility data from supersaturated conditions. To obtain

data from undersaturated conditions, the authors titrated the systems down in pH with the addition of 0.1 M $HClO_4$. In calculating the K_{sp}, the authors accounted for aqueous uranyl complexation; however, they did not account for ionic strength effects. Consequently, their solubility measurements yielded conditional $\lg K_{sp}$ value of (5.72 ± 0.19) at 0.1 M ionic strength, which is the average of results from the 0.03% and 0.98% CO_2 atmospheres. In a subsequent study using the same techniques, Meinrath *et al.* [22] again calculated the K_{sp} of metaschoepite using solubility measurements for systems with 0.03% and 0.3% CO_2 atmospheres. They used single ion activity coefficients of $10^{-0.40}$, $10^{-0.46}$, and $10^{-0.09}$ for UO_2^{2+}, CO_3^{2-}, and H^+, respectively, to calculate activities and again accounted for aqueous uranyl complexation; however, there is no comment on the origin of the activity coefficient values. Their reported $\lg K_{sp}$ values are (5.14 ± 0.05) and (4.68 ± 0.14) for 0.03% and 0.3% CO_2 atmospheres, respectively.

Arocas and Grambow [34] measured the separate solubilities of metaschoepite and a sodium polyuranate ($Na_{0.33}UO_{3.16}(H_2O)_2$), with each phase precipitated from supersaturated solutions of UO_2Cl_2 in 0.5 M $NaClO_4$, 3 M NaCl, or 5 M NaCl. Titration of the experimental systems from pH 4.7 to 8.9 induced precipitation. The authors obtained one set of solubility data from undersaturation by allowing the pH 4.7 systems to reach equilibrium from supersaturation, and then they replaced most of the solution with fresh $NaClO_4$ electrolyte to gather data from undersaturated conditions. XRD analysis of the solid phases from the 0.5 M $NaClO_4$ system confirmed the solid phase was metaschoepite, while the 3 and 5 M NaCl systems identified the solids as sodium polyuranate. Using the Pitzer equations to calculate uranyl activities, and taking into account aqueous uranyl complexation, the authors produced $\lg K_{sp}$ values for metaschoepite and sodium polyuranate of (5.37 ± 0.25) and (7.13 ± 0.15), respectively.

Because of the prevalence of Ca-bearing pore and groundwaters in possible nuclear waste repository settings [35], a number of studies have measured the solubility of synthetic becquerelite ($Ca(UO_2)_6O_4(OH)_6(H_2O)_8$), yielding calculated $\lg K_{sp}$ values ranging from 41.2 to 44.7. The variability in the measurements may be due to differences in the crystallinity of the mineral phase used in each experiment. Solubility measurements using a natural becquerelite sample produced a much lower $\lg K_{sp}$ of (29) [36]. Presumably the natural becquerelite crystal has a higher degree of crystallinity than synthetic powders, and lower crystallinity materials typically exhibit significantly higher solubilities (*e.g.* [37]). These studies are described in more detail below.

Sandino *et al.* [38] measured the solubility of synthetic becquerelite from undersaturated conditions with respect to U. One set of experiments involved using synthetic metaschoepite (the metaschoepite conversion experiment) in 1 m $CaCl_2$, and the other started with synthetic becquerelite in 1 m $CaCl_2$. With thorough characterization of the mineral phases by XRD, XPS, and scanning electron microscopy and energy dispersive spectroscopy (SEM-EDS), Sandino *et al.* [38] demonstrated that in their experiments the metaschoepite converted to becquerelite which subsequently equilibrated with the solution. The experiment that started with becquerelite as the initial phase did not undergo alteration as the mineral phase equilibrated with the solution; however, there was some reduction in the crystallinity of the phase that they did not observe with the metaschoepite conversion experiment. Using the SIT-BGS approach to calculate uranyl activities while accounting for aqueous uranyl complexation these experiments yielded $\lg K_{sp}$ values of (41.89 ± 0.52) and (43.70 ± 0.47) for the metaschoepite conversion experiment and the becquerelite experiment, respectively. The authors suggest that the variation in the K_{sp} value from the experiments is likely due to differing degrees of crystallinity of the synthetic solids. This interpretation is reasonable because the lower degree of crystallinity material (in the becquerelite experiment) yielded a higher measured solubility. A ripening process, thereby producing a higher crystallinity becquerelite and consequently a lower solubility, may have affected the metaschoepite conversion experiment.

Vochten *et al.* [39] also measured the solubility of becquerelite from undersaturation with respect to U. The authors characterized the mineral phase prior to the solubility experiments using a range of analytical approaches including bulk phase analysis by atomic absorption spectroscopy (AAS), XRD, and TGA. It is unclear if the solid phase was checked for alteration after the experiments. The mineral phase was allowed to equilibrate in water for 1 week under a range of pH conditions from 4.5 to 6.3. Calcium and pH were the only measurements made on the equilibrated solution. The authors assumed stoichiometric dissolution, although not verified by any technique, to obtain uranyl concentrations and to calculate the $\lg K_{sp}$ value of (43.2 ± 0.3). The ionic strength of the experiment was not specified nor was it apparent that any corrections for ionic strength were made; however, the authors did take into account aqueous uranyl complexation when calculating the $\lg K_{sp}$. This value must be considered as a conditional constant at best.

Rai *et al.* [35] conducted their experiments on the solubility of becquerelite exclusively from undersaturated conditions under a N_2 atmosphere. The experimental solutions initially contained 0.02 to 0.5 M $CaCl_2$. Post experimental residues, characterized by XRD, verified the presence of becquerelite in addition to other minor peaks that became more pronounced at higher pH. Chemical analysis of post-experimental residues below pH 8 produced molar ratios of U:Ca similar to that of becquerelite (6:1); however, U:Ca ratios in residues from experiments above pH 8 decreased to approximately 2. This decrease in U:Ca coincides with the likely formation of $CaUO_4$ and $Ca_2UO_5(H_2O)_{1.3-1.7}$, the most likely phases to form under alkaline conditions in the presence of Ca and U [40]. The authors used Pitzer equations to calculate uranyl activities while accounting for aqueous uranyl complexation. Using the solubility data obtained from the lowest ionic strength system (0.02 M)

from pH 4.5 to 7, the authors calculated a $\lg K_{sp}$ of (41.2 ± 0.2).

Casas *et al.* [36] measured the solubility of a natural becquerelite sample. The becquerelite crystals were characterized by optical microscopy, electron microprobe analysis (EMPA), SEM, EDS, and XRD. Becquerelite crystals were washed with double distilled water (DDI), and placed in a vessel with fresh DDI water in order to enable the system to equilibrate initially from undersaturated conditions. Once a steady state was reached, the pH of the system was adjusted and left to reach a new steady state under the new pH conditions. By adjusting the pH appropriately, the authors obtained data from supersaturation and undersaturation. Examining the post-experimental mineral residue with XRD and SEM revealed no precipitation of schoepite, but a minor component (less than 5%) of soddyite was identified. The authors suggest the soddyite came from the transformation of uranophane ($Ca[(UO_2)(SiO_3OH)]_2(H_2O)_5$), which was associated with some becquerelite crystals. Using the SIT-BGS approach to calculate uranyl activities and accounting for aqueous uranyl complexation, the resulting $\lg K_{sp}$ value from these experiments was (29 ± 1). The authors suggest that the drastically lower K_{sp} value that they obtain relative to other solubility studies with synthetic becquerelite is due to the higher degree of crystallinity of the natural sample.

Perhaps one of the most important uranyl oxide hydrate minerals in terms of spent nuclear fuel alteration is the sodium analogue of compreignacite ($Na_2(UO_2)_6O_4(OH)_6(H_2O)_8$ [41]). Dissolved sodium in the groundwater at a geologic repository site, and/or significant release of sodium from waste-containing glass at the site, may influence the mineral phases formed during the alteration of spent fuel [4,42,43]. In addition to the sodium end-member phase, it is also important to have solubility data for the potassium end member as well as for mixed potassium–sodium phases in order to understand solid-phase cation effects on the solubility. Mixed potassium–sodium data in conjunction with end-member data enable the calculation of an activity coefficient for the mineral phase, thereby permitting predictions of the solubility of mixed phases with potassium:sodium ratios not directly studied in the laboratory.

Unfortunately, solubility data for these sodium and potassium uranyl oxide hydrate phases are sparse. Only one study reports a measured solubility of compreignacite ($K_2(UO_2)_6O_4(OH)_6(H_2O)_8$), and no published solubility measurements exist for its sodium analogue. Sandino *et al.* [38] measured the solubility of a synthetic compreignacite by means of two different types of experiments. One experiment involved starting with synthetic metaschoepite (the metaschoepite conversion experiment) in 1 m KCl, and the other experiment involved starting with synthetic compreignacite in 1 m KCl. Mineral phase characterization by XRD, XPS, and scanning electron microscopy and energy dispersive spectroscopy (SEM-EDS) indicated that metaschoepite converted fully to compreignacite during the experiment. The same analyses conducted on the solids in the experiment that initially started with compreignacite revealed no alteration of the mineral phase; however, there was evidence of a reduction in the crystallinity. The solubility measurements were conducted from undersaturated conditions with respect to U. Using the SIT-BGS approach to calculate uranyl activities and accounting for aqueous uranyl complexation, the authors calculated $\lg K_{sp}$ values of (36.82 ± 0.32) and (39.16 ± 0.31) for the metaschoepite conversion experiment and the compreignacite experiment, respectively. Similar to their becquerelite results, Sandino *et al.* [38] attribute the difference in the K_{sp} values to the differing degrees of crystallinity of the solid phases. The metaschoepite conversion experiment likely underwent a ripening effect that increased the crystallinity of the phase and thus produced a lower calculated K_{sp}.

Giammar and Hering [44] measured the kinetics of soddyite dissolution in a $NaNO_3$ electrolyte. During the course of their experiments, they analyzed the solid phase at every sampling point with XRD, SEM, and Raman spectroscopy. The solid phase analyses revealed the formation of a clarkeite-like sodium uranyl oxide hydrate phase that ultimately was the likely solubility-controlling phase. In order to calculate a K_{sp} value for the clarkeite-like phase, the authors needed to account for soddyite dissolution in their experiments. To do this, they used a recalculated value of the soddyite K_{sp} from Nguyen *et al.* [45] described below. To calculate uranyl activities and account for ionic strength effects in their experiments, the authors used the Davies equations and took into account aqueous uranyl complexation by hydroxide and carbonate. This produced a $\lg K_{sp}$ of (9.02) for the clarkeite-like phase from data gathered from supersaturation. No errors are reported for this value since the purpose of this study was not to measure the solubility of the clarkeite-like sodium uranyl oxide hydrate phase.

A wide range of experimental techniques have been used to measure the solubility of uranyl oxide hydrates, including conversion experiments, batch experiments, and precipitation experiments. Our review indicates that these experimental techniques can yield solid phase experimental products with dramatically different crystallinities, and that the crystallinity of the mineral phase can, in turn, dramatically affect the measured solubility of the phase. Very few studies have conducted solubility measurements from both supersaturated and undersaturated conditions, and post-experimental residue analyses have also varied greatly or have been absent. Crystallinity (see discussion below) and the lack of rigorous demonstrations of equilibrium (steady state attained from supersaturated and undersaturated conditions) are likely the main causes in the variability of the calculated K_{sp} values. Table 1 illustrates the wide range of K_{sp} values reported for the oxide hydrates. In addition to the phases discussed here, the solubility of a number of other environmentally relevant uranyl oxide hydrate phases have yet to be measured, such as the sodium analogue of compreignacite, mixed sodium–potassium compreignacite, β-$UO_2(OH)_2$, $CaUO_4$, and $Ca(UO_2)_6O_4(OH)_6(H_2O)_8$.

3.3. Uranyl silicates

Studies of natural analogues and laboratory experiments indicate that uranyl silicates are likely to be the final uranyl mineral phases formed in the paragenetic alteration of spent nuclear fuel under oxidizing conditions when dissolved silica is present [4]. In general, the uranyl silicates are less soluble than uranyl carbonates or uranyl oxide hydrates under circumneutral pH conditions; therefore, they are likely to serve as controls on the aqueous phase concentrations of U. In addition to the importance of uranyl silicates in repository environments, sodium boltwoodite has been identified in the vadose zone of the contaminated sediment at Hanford [7]. Uranyl silicates are of paramount importance in determining the mobility of U in subsurface conditions where dissolved silica is present.

In order to illustrate the difference in typical solubilities of uranyl silicates, uranyl oxide hydrates, and uranyl phosphates, a calculation presented in figure 1 describes the solubility of uranyl orthophosphate, metaschoepite, and sodium boltwoodite ($Na[UO_2(SiO_3OH)](H_2O)_{1.5}$) in the presence of 10 mM Na^+ and $pCO_2 = 32$ Pa. For accurate comparison of the solubilities, calculations take into account the same aqueous complexation reactions for each system (reactions listed in table 2). The solubility of each uranyl phase considered increases dramatically at higher pH due to the predominance of aqueous uranyl carbonate complexes that become important under these conditions. Below approximately pH 8, uranyl orthophosphate is much less soluble than either of the other phases. For example, at pH 6, the solubility difference is approximately 3.5 orders of magnitude. Above pH 8, although aqueous uranyl carbonate complexation affects both solubilities, uranyl orthophosphate becomes more soluble than sodium boltwoodite. Sodium boltwoodite solubility at low pH conditions is higher than that of metaschoepite due to the formation of an aqueous uranyl silicate species, $UO_2H_3SiO_4^+$, that is prevalent below pH 6 and is negligible under higher pH conditions (and is absent in the Si-free systems). Clearly, pH, uranyl mineralogy, dissolved CO_2 concentration, and aqueous uranyl complexation all exert controlling influences on U mobility and transport through solubility relationships. Uranyl silicates can represent the phases that control subsurface U concentrations under circumneutral to basic groundwater conditions.

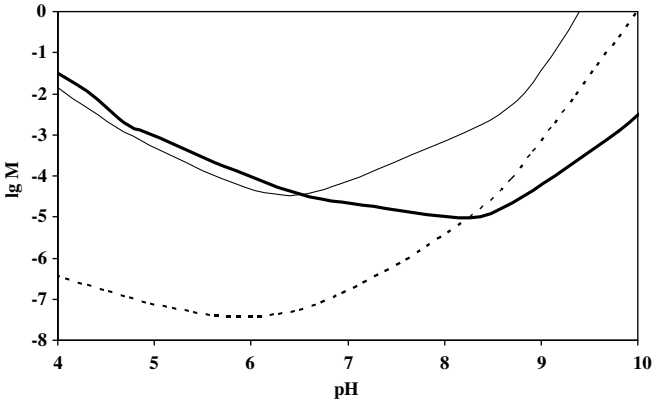

FIGURE 1. Plot of logarithm of total U in solution against pH for the calculated solubility of sodium boltwoodite (thick solid curve), metaschoepite (thin solid curve), and uranyl orthophosphate (dashed curve) in the presence of 10 mM Na^+ and $pCO_2 = 32$ Pa. The predicted solubilities take into account reactions listed in Table 2 and mineral $\lg K_{sp}$ values from [31,32,47].

TABLE 2
Aqueous complexation reactions

	$\lg K\ (I = 0)$	Reference
$UO_2^{2+} + H_2O = UO_2OH^+ + H^+$	−5.25	[12]
$UO_2^{2+} + 2H_2O = UO_2(OH)_2^\circ + 2H^+$	−12.15	[12]
$UO_2^{2+} + 3H_2O = UO_2(OH)_3^- + 3H^+$	−20.25	[12]
$UO_2^{2+} + 4H_2O = UO_2(OH)_4^{2-} + 4H^+$	−32.4	[12]
$2UO_2^{2+} + H_2O = (UO_2)_2OH^{3+} + H^+$	−2.70	[12]
$2UO_2^{2+} + 2H_2O = (UO_2)_2(OH)_2^{2+} + 2H^+$	−5.62	[12]
$3UO_2^{2+} + 5H_2O = (UO_2)_3(OH)_5^+ + 5H^+$	−15.55	[12]
$3UO_2^{2+} + 7H_2O = (UO_2)_3(OH)_7^- + 7H^+$	−32.20	[12]
$4UO_2^{2+} + 7H_2O = (UO_2)_4(OH)_7^+ + 7H^+$	−21.90	[12]
$UO_2^{2+} + CO_3^{2-} = UO_2CO_3$	9.94	[12]
$UO_2^{2+} + 2CO_3^{2-} = UO_2(CO_3)_2^{2-}$	16.61	[12]
$UO_2^{2+} + 3CO_3^{2-} = UO_2(CO_3)_3^{4-}$	21.84	[12]
$3UO_2^{2+} + 6CO_3^{2-} = (UO_2)_3(CO_3)_6^{6-}$	54.00	[12]
$2UO_2^{2+} + CO_3^{2-} + 3H_2O = (UO_2)_2CO_3(OH)_3^- + 3H^+$	−0.86	[12]
$3UO_2^{2+} + CO_3^{2-} + 3H_2O = (UO_2)_3O(OH)_2(HCO_3)^+ + 3H^+$	0.65	[12]
$11UO_2^{2+} + 6CO_3^{2-} + 12H_2O = (UO_2)_{11}(CO_3)_6(OH)_{12}^{2-} + 12H^+$	36.40	[12]
$UO_2^{2+} + H_4SiO_4 = UO_2H_3SiO_4^+ + H^+$	−1.84	[12]
$Si(OH)_{4(aq)} = 2H^+ + SiO_2(OH)_2^{2-}$	−23.14	[12]
$Si(OH)_{4(aq)} = H^+ + SiO_2(OH)_3^-$	−9.81	[12]
$2Si(OH)_{4(aq)} = Si_2O_3(OH)_4^{2-} + 2H^+ + H_2O$	−19.0	[11]
$2Si(OH)_{4(aq)} = Si_2O_2(OH)_5^- + H^+ + H_2O$	−8.1	[11]
$3Si(OH)_{4(aq)} = Si_3O_6(OH)_3^{-3} + 3H^+ + 3H_2O$	−28.6	[11]
$3Si(OH)_{4(aq)} = Si_3O_5(OH)_5^{-3} + 3H^+ + 2H_2O$	−27.5	[11]
$4Si(OH)_{4(aq)} = Si_4O_7(OH)_5^{-3} + 3H^+ + 4H_2O$	−25.5	[11]
$4Si(OH)_{4(aq)} = Si_4O_8(OH)_4^{-4} + 4H^+ + 4H_2O$	−36.3	[11]
$Na^+ + CO_3^{2-} = NaCO_3^-$	−1.27	[86]
$Na^+ + CO_3^{2-} + H^+ = NaHCO_3^\circ$	−10.03	[86]
$Ca^{2+} + UO_2^{2+} + 3CO_3^{2-} = CaUO_2(CO_3)_3^{2-}$	27.18	[75]
$2Ca^{2+} + UO_2^{2+} + 3CO_3^{2-} = Ca_2UO_2(CO_3)_3^\circ$	30.70	[75]

Nguyen *et al.* [45] performed individual solubility experiments from undersaturated conditions with soddyite, uranophane ($Ca(H_3O)(UO_2)_2(SiO_4)_2(H_2O)_3$ later refined and reported as $Ca[(UO_2)(SiO_3OH)]_2(H_2O)_5$ [46]), Na-boltwoodite ($NaH_3OUO_2SiO_4(H_2O)$ later refined and reported as $Na[UO_2(SiO_3OH)](H_2O)_{1.5}$ [42]), and Na-weeksite ($Na_2(UO_2)_2(Si_2O_5)_3(H_2O)_4$) at $T = 303.15$ K. Pre-experimental characterization of the mineral phases involved XRD, FTIR, and chemical analysis (hereafter referred to as bulk dissolution analysis) involving dissolution of the phase in an acidic solution and subsequent analysis by AAS. The pre-experimental characterization indicated that Na-boltwoodite and Na-weeksite were pure phases; and the elemental ratios of the solids indicated that amorphous silica was likely present with the soddyite and uranophane. Post-experimental analysis of the mineral residues by XRD

indicated that soddyite and Na-weeksite were stable but a few minor peaks were missing likely due to preferred orientation of the solid phase. The XRD of the uranophane residue indicated no alteration. The Na-boltwoodite residue confirmed that Na-boltwoodite was still present; however, new peaks were present in the sample that corresponded to the major peaks found in soddyite. The solubility experiments resulted in non-stoichiometric dissolution of each mineral phase examined. Specifically, the silica concentrations in all samples were close to the amorphous silica solubility limit, and there was excess Na present in the systems containing Na-boltwoodite and Na-weeksite. Using the SIT-BGS approach to calculate uranyl activities and accounting for aqueous uranyl complexation, Nguyen *et al.* [45] calculated $\lg K_{sp}$ values for soddyite, uranophane, Na-boltwoodite, and Na-weeksite of (5.74 ± 0.21), (9.42 ± 0.48), (5.82 ± 0.16), and (1.50 ± 0.08), respectively. The Na-boltwoodite value is a lower bound due to the formation of soddyite during the experiment. The lack of reversibility of these experiments makes it impossible to assess whether the quoted uncertainties associated with the K_{sp} values are reasonable or not.

Ilton *et al.* [47] measured the dissolution of Na-boltwoodite under a variety of conditions. They performed kinetics experiments, 7-day experiments, and pre-treated experiments. All measurements were made in a 50 mM $NaNO_3$ buffer. The kinetics experiments were performed as a function of $NaHCO_3$ concentration from 0.1 mM to 50 mM. At 50 mM $NaHCO_3$, additional experiments were performed varying the solid:solution ratio from 0.5 g/100 ml to 1.0 g/100 ml. The 7-day experiments were only sampled after seven days of mineral–solution interaction, and had $NaHCO_3$ concentrations from 0 mM to 50 mM. The pre-treated experiments were a subset of the kinetics experiments, and involved preleaching of the mineral in a 50 mM bicarbonate solution for 24 h. Under certain initial conditions, the authors observed congruent dissolution; however, under all experimental conditions, dissolution eventually became incongruent. The authors were not able to identify the phase or cause of the incongruent dissolution because the XRD patterns of the post-experimental residues did not exhibit any new peaks. Despite the existence of an unidentified and likely amorphous alteration phase that grew during the experiments, Ilton *et al.* [47] calculated the $\lg K_{sp}$ value for Na-boltwoodite using final data points from eight experiments that clearly manifested a steady state, and using data points from two other experiments that were near steady-state conditions. Accounting for aqueous uranyl complexation and using the Pitzer ion interaction model and the Davies equation to calculate activity coefficients, the calculated $\lg K_{sp}$ values were (5.86 ± 0.24) and (5.85 ± 0.26), respectively.

Casas *et al.* [48] performed solubility experiments using natural samples that primarily consisted of uranophane but also contained a range of other mineral phases. No effort was made to separate these mineral phases, and consequently each experiment had different potential controls on element concentrations in solution. Solubility experiments performed under an N_2 atmosphere under circumneutral pH conditions produced highly scattered data. Post-experimental analysis of the solids consisted of SEM and EDS, and revealed mineral phases in addition to uranophane with habits similar to schoepite and rutherfordine. The authors used two different methods to calculate a K_{sp} for uranophane from the experimental data. The first treatment assumed stoichiometric dissolution despite the analytical data that clearly demonstrated a deviation from this stoichiometry; the second data treatment solved for a K_{sp} value for each experimental sample, instead of just the final one or the steady-state samples, and accounted for the presence of uranyl hydroxide aqueous species in solution. In both data treatments, activity coefficients were neglected. The two data treatments produced $\lg K_{sp}$ values of (6.5 no error reported) and (7.8 ± 0.8), respectively. The second data treatment was more rigorous than the first; however, the scatter in the data, the assumption that uranophane was the solubility controlling phase, and ignoring activity coefficients in the calculations make the calculated K_{sp} values from both treatments highly unreliable.

Perez *et al.* [49] measured the extent of dissolution of uranophane in (1 to 20) mM bicarbonate solutions. The solid material was characterized prior to the solubility experiments with XRD, BET, and bulk dissolution analysis. Post-experimental XRD analyses showed no signs of alteration of the mineral phase. The authors assumed stoichiometric dissolution of the mineral as verified by a limited number of analyses of Ca and Si; however, U concentrations in solution decreased after *ca.* 300 h, and the calculated K_{sp} value for each data point in the experiments decreased with increasing bicarbonate concentrations, both effects likely due to the precipitation of a secondary uranyl phase. Despite this possibility and the lack of evidence of a secondary phase in the mineral residue, the authors included these lower K_{sp} values when determining an overall averaged $\lg K_{sp}$ for uranophane of (11.7 ± 0.6) using the SIT-BGS approach to calculate activities and accounting for aqueous uranyl complexation. Their calculated K_{sp} value is not well constrained due to lack of Ca and Si analyses for every data point, the un-validated assumption of stoichiometric dissolution, and the likely presence of a secondary phase during at least a portion of the experiments.

Moll *et al.* [50] measured the solubility of soddyite from undersaturated conditions in air and in a N_2 atmosphere from pH 3 to 9. Using XRD analysis, the authors did not detect any secondary phase formation in the solid in equilibrium with the final aqueous solution, yet during the course of the experiment, after the initial increase of U in solution from the dissolution of soddyite there was a notable decrease in the U concentration in solution, likely caused by the formation of a secondary sodium uranyl silicate and/or a uranyl carbonate phase. The fact that there was no evidence of a secondary phase in the final mineral

residue characterized by XRD highlights the relative insensitivity of XRD analysis compared to analyses of the aqueous elemental concentrations as a function of time. Above pH 4.6, aqueous uranyl hydroxide complexes and uranyl carbonate complexes are a sufficient proportion of the total dissolved U that they must be considered when determining K_{sp} values. Moll *et al.* [50] used data from the pH 3 experiments only and the SIT-BGS approach to calculate uranyl activities to produce $\lg K_{sp}$ values of (6.03 ± 0.45) and (6.15 ± 0.53) from the data from the air and the N_2 experiments, respectively. While these values are not constrained by data from supersaturation, they are within error of the previous measurements by Nguyen *et al.* [45].

The most recent measurement of soddyite solubility, by Gorman-Lewis *et al.* [13], used a synthetic solid phase, and attained equilibrium from supersaturated and undersaturated conditions between pH 3 and 4. Aqueous uranyl and silica were added to the experimental solutions prior to contact with the mineral phase in order to decrease the time required to attain steady-state conditions. Amorphous silica was also added in excess to buffer the aqueous silicon concentration and to decrease the equilibration time. Pre- and post-experimental characterizations using XRD, FTIR, and chemical analysis revealed that the soddyite and amorphous silica appeared to remain stable throughout the course of the experiments. The authors used an extended Debye–Huckel equation to calculate uranyl activities while taking into account aqueous complexation of uranyl to produce a $\lg K_{sp}$ value of $(6.43\ +0.2/-0.37)$. While this value is higher than the previous measurements, it does fall within the error of the values calculated by Moll *et al.* [50], and it is the only value constrained by data from supersaturation as well as undersaturation.

The uranyl silicates are important minerals in terms of geologic repository performance, yet their solubilities in general remain poorly constrained. Soddyite and Na-boltwoodite are the only uranyl silicates for which well-constrained solubility measurements exist. As is the case for the uranyl oxide hydrates, data from well characterized mixed cation phases of sodium/potassium weeksite and boltwoodite would enable calculations of activity coefficients for these solid phases which would allow for determination of solubilities along the whole solid-solution series of mineral families. In addition to the uranyl silicates identified in this review, other environmentally relevant silicates for which no solubility data are available include kasolite ($Pb(UO_2)(SiO_4)H_2O$), slodowskite ($Mg[(UO_2)(SiO_3OH)]_2(H_2O)_6$), and haiweeite ($Ca(UO_2)_2(Si_2O_5)_3(H_2O)_5$).

3.4. Uranyl phosphates

Uranyl phosphates, due to their extremely low solubilities under circumneutral pH conditions, are important phases for controlling U mobility in the environment. Murakami *et al.* [5] identified saleeite ($Mg(UO_2)_2(PO_4)_2(H_2O)_{10}$) and metatorbenite ($Cu(UO_2)_2(PO_4)_2(H_2O)_8$) as the controlling phases for dissolved U in the vicinity of the secondary ore deposit at the U ore deposit in Koongarra, Australia. Autunite largely controls the mobility of U in soils contaminated by actinides, such as at the Fernald site in Ohio [51], where U was processed during the Cold War, and the U-contaminated K1300 locality of the DOE-K 25 site at Oak Ridge, Tennessee [8]. Autunite-group minerals are bioprecipitated by *Citrobacter* sp., which is proposed for remediation of groundwater contaminated by heavy metals [52,53]. They have been found in experiments involving halophilic bacterium isolated from the Waste Isolation Pilot Plant repository [9,10]. Autunite-group minerals precipitate at reactive barriers that use phosphate to limit the transport of U in groundwater [54,55], and their stabilities under vadose and saturated-zone conditions will determine the long-term effectiveness of these remediation strategies.

Uranyl phosphates are sparingly soluble; therefore, solubility experiments are typically performed under acidic conditions at high ionic strength to induce enough dissolution for detection of the dissolved species. A difficulty with measurements performed at high ionic strength is the extrapolation to infinite dilution in order to calculate the K_{sp} value. For environmental applications uranyl phosphate solubility predictions under circumneutral conditions are desirable; however, without K_{sp} values extrapolated to infinite dilution, measurements that are conducted under acidic conditions cannot be reliably applied to the circumneutral pH and low ionic strength conditions often found in the environment. Another issue with uranyl phosphate solubility measurements involves the aqueous uranyl-phosphate complexation, which must be taken into account when calculating K_{sp} values from these experiments. An advantage of the sparingly soluble phases is the ease of gathering data from supersaturated conditions or precipitation experiments due to the fast kinetics of the precipitation reaction. Below we have summarized studies measuring the solubility of potentially environmentally-important uranyl phosphates.

Vesely *et al.* [56] measured the solubility of uranyl hydrogen phosphate also known as chernikovite ($UO_2HPO_4(H_2O)_4$), uranyl orthophosphate ($(UO_2)_3(PO_4)_2(H_2O)_4$), and $MUO_2PO_4(H_2O)_x$, where $M = Na^+$, K^+, Rb^+, Cs^+, NH_4^+. Syntheses involved combining uranyl nitrate, phosphoric acid, and the appropriate nitrate salt. Characterization of the solids consisted of two approaches: (1) bulk dissolution analysis and (2) water of crystallization analysis determined by weight loss upon drying. There is no mention of using XRD to verify the crystallinity and identity of the synthetic phases. Post-experimental solid analysis is not mentioned. Solubility experiments involved measuring aqueous cation concentrations in experiments from undersaturated conditions in solutions from pH 0.7 to 2.1 with ionic strengths ranging from 0.22 M to 0.32 M. The authors considered the formation of aqueous uranyl phosphates when calculating the $\lg K_{sp}$ values listed in table 1; however, they did not extrapolate their values to infinite dilution.

Another study measuring the solubility of uranyl hydrogen phosphate and uranyl orthophosphate by Markovic *et al.* [57] conducted experiments in which equilibrium was approached from supersaturated conditions by precipitating the solids from solutions containing uranyl nitrate and phosphoric acid. Examination of the samples took place after 30 days and produced data from pH 1.41 to 3.17. The ionic strengths in the experimental systems are reported to have varied from 3 mM to 39 mM, although considering the H^+ activities alone at the experimental pH values, the reported ionic strength values at low pH must be higher than 39 mM. Characterization of the solid phases involved XRD, IR, and optical microscopy. The authors did account for uranyl complexation by phosphate and calculated K_{sp} values, extrapolated to infinite dilution using the Davies equation, of (-12.33 ± 0.06) and (-49.00 ± 0.80) for uranyl hydrogen phosphate and uranyl orthophosphate, respectively. In a later study, Markovic *et al.* [58] measured the solubility of $NH_4UO_2PO_4(H_2O)_3$ in a similar manner as the previously described study by precipitating the solids from a uranyl nitrate, phosphoric acid, and ammonium hydroxide. The authors examined the samples after 30 days with XRD, IR, TGA, and chemical analysis by gravimetric, spectrophotometric, and chemical mircoanalysis techniques. Their precipitation technique gathered data from pH 1.23 to 1.76. Accounting for aqueous uranyl complexation and calculating aqueous ion activity coefficients using the Davies equation, their calculated $\lg K_{sp}$ is (-26.50 ± 0.09).

Unlike previous measurements of uranyl orthophosphate ($(UO_2)_3(PO_4)(H_2O)_4$), Sandino *et al.* [31] measured its solubility over a wide pH range from 3 to 9. Characterization of the solid before and after the solubility experiments with XRD, TGA, BET, SEM, and chemical analysis involving acid digestion of the phase and subsequent analysis of the solution indicated that it was uranyl orthophosphate and did not undergo alteration during the course of the experiments. The authors added the solid phase to a solution containing 0.5 M $NaClO_4$ and a constant phosphate concentration of 0.01 M PO_4^{3-}, used to stabilize the phase. Titrating the suspension as a function of the acidity, the acid/base used to vary the acidity was not specified, the authors measured dissolved U and P concentrations, assuming that a steady state was attained at each step when the potential of the glass electrode remained constant within 0.1 mv for 24 h. In the circumneutral pH range, the solubility of uranyl phosphates is extremely low; consequently, the authors used a laser fluorescence analyzer with a detection limit of $2.1 \cdot 10^{-10}$ M for U analyses. Accounting for aqueous uranyl complexation with phosphate, hydroxide, and carbonate, and extrapolating to infinite dilution using the SIT-BGS approach, the authors calculated a $\lg K_{sp}$ value of (-53.32 ± 0.17).

Rai *et al.* [59] also measured the solubility of uranyl orthophosphate from undersaturation and, similar to that of Sandino *et al.* [31], the study also encompassed a wide pH range (2.5 to 10); however, the authors also used a wide phosphate concentration range (0.0001 to 1) M. Pre-experimental mineral phase characterization included XRD, differential thermal analysis (DTA), TGA, and X-ray absorption spectroscopy (XAS). Post-experimental characterization by XRD and XAS was only performed on select samples. The authors let samples equilibrate for (29 to 870) days. Steady-state aqueous concentrations achieved after 29 days were similar to those measured at 870 days. The authors accounted for aqueous uranyl speciation and used the Pitzer model to calculate activity coefficients to produce a $\lg K_{sp}$ of (-49.08 ± 0.48).

Pavkovic *et al.* [60] measured the solubility of $KUO_2PO_4(H_2O)_3$ by precipitating the phase from supersaturated solutions that were created by holding uranyl ion concentration constant at 1 mM with uranyl nitrate and varying the concentrations of H_3PO_4 and KOH. The pH of the systems varied from 1.5 to 2. After a 30 day aging period, characterization of the solids involved XRD, SEM, TGA, and bulk dissolution analysis. The initial and final solid phase was determined to be $KUO_2PO_4(H_2O)_3$. Using spectrophotometric techniques to analyze for U and P, and flame photometry techniques to analyze for K^+, the authors calculated a $\lg K_{sp}$, extrapolated to infinite dilution using the Davies equation, of (-26.28 ± 0.25) taking into account aqueous uranyl speciation.

Solubility measurements of chernikovite and meta-ankoleite ($K(UO_2)(PO_4)(H_2O)_3$), conducted by Van Haverbeke *et al.* [61], yielded conditional K_{sp} values from solution concentrations (not activities) of (-22.72 ± 0.24) and (-24.30 ± 0.81), respectively. Pre-experimental solid phase analysis consisted of XRD, TGA, SEM, IR, and fluorescence spectroscopy. Solubility measurements, performed under a nitrogen atmosphere from pH 1 to 2.2, produced data from undersaturated conditions by adding mineral to a solution of distilled water with the pH adjusted using $HClO_4$. Sampling occurred every 5 days and a steady state was attained after 30 days. Post-experimental residue analysis with XRD and an undescribed chemical analysis revealed the presence of a precipitate in the meta-ankoleite experiment identified as $(UO_2)_3(PO_4)_2$. The authors made no attempt to correct the solution concentrations for ionic strength, claiming that the ionic strength of the solutions was too high (the ionic strengths of the solutions were not specified) for making accurate activity coefficient calculations.

Uranyl phosphates are an extremely important group of uranyl minerals when considering U sequestration. Conditional K_{sp} values can only be used to yield rough approximations of the solubility behavior and relative stabilities of these minerals under environmentally relevant conditions; therefore, extrapolation of K_{sp} values to infinite dilution is essential. In addition to the importance of extrapolation to infinite dilution, constraining the K_{sp} by gathering data from both supersaturated and undersaturated conditions is also essential and also lacking from the reviewed studies. Uranyl phosphates that may be important sequestration phases for contaminated sites that are lacking solubility measurements are saleeite, metatorbenite,

bassetite ($Fe^{2+}(UO_2)_2(PO_4)_2(H_2O)_{8-12}$), autunite ($Ca(UO_2)_2(PO_4)_2\ (H_2O)_{8-10}$), and meta-autunite ($Ca(UO_2)_2(PO_4)_2(H_2O)_{6-8}$).

3.5. Uranyl peroxides

The uranyl peroxide minerals studtite ($((UO_2)O_2(H_2O)_4)$) and metastudtite ($UO_4(H_2O)_2$) form in U deposits due to the accumulation of peroxide created by alpha-radiolysis of water [62]. There is also evidence that uranyl peroxides may be important alteration products of nuclear wastes under environmental conditions. McNamara *et al.* [63] found that studtite formed on the surface of spent nuclear fuel reacted at $T = 298$ K with de-ionized water for 1.5 years and suggested it grew by incorporating peroxide created by alpha-radiolysis of water. Metastudtite formed on the surface of UO_2 under irradiation with a $^4He^{2+}$ (alpha-particle) beam, and incorporated peroxide formed by alpha-radiolysis of water [64]. Studtite has also been found on nuclear material ("lava") following the Chernobyl Nuclear Plant accident [65].

Djogić *et al.* [66] measured the solubility of metastudtite by precipitation from solutions of $UO_2(ClO_4)_2$ and H_2O_2. The authors created a precipitation boundary by varying the concentrations of uranyl and H_2O_2 and monitoring precipitation via a tyndallometer in combination with a photometer. To hold the ionic strength constant the authors buffered the system with 0.7 M $LiClO_4$ and the pH of all experimental solutions at the end of the experiments was 4.6. Varying the solution compositions affected the kinetics of precipitation; consequently, the authors chose to use the solubility data for their K_{sp} value from the systems with an excess of H_2O_2 which caused precipitation to occur within 3 days. Characterization of the precipitate with XRD and TGA confirmed its identity as metastudtite. The authors calculated the free uranyl and O_2^{2-} from the precipitation boundary, taking into account uranyl complexation by hydroxide and the dissociation of H_2O_2. K_{sp} calculations did not take into account ionic strength effects; therefore, the authors K_{sp} value of (-35.88 ± 0.01) is only valid at 0.7 M ionic strength.

Kubatko *et al.* [62] measured the solubility of studtite by titrating uranyl solutions (the anion of the salt was not specified) with H_2O_2 until a precipitate formed. The data encompassed the pH range of 2.91 to 3.37, and characterization of the precipitate involved XRD analysis. The authors did not take into account uranyl complexation by O_2^{2-} or OH^-, although, complexation is unlikely under the conditions of the experiments. The ionic strength of the system is unspecified, and the authors do not account for ionic strength effects in their solubility calculations. Their reported $\lg K_{sp}$ values range from (−2.88) to (−2.86).

The K_{sp} values from the uranyl peroxide studies described require further refinement due to the lack of accounting for ionic strength effects and the lack of reversibility experiments. These studies provide an estimate of the solubility of metastudtite and studtite under a relatively restricted range of conditions; however, due to the environmental relevance of these phases more rigorous solubility studies are necessary in order to evaluate the importance of uranyl peroxide phases on U mobility under more environmentally relevant conditions.

3.6. Uranyl sulfates

Uranyl sulfates are relatively widespread, although not abundant [67]. They usually occur close to actively oxidizing uraninite and sulfide minerals. They commonly occur in sites mined for U, where they form due to the evaporation of acid sulfate-rich mine drainage waters [41,68]. These minerals usually occur as fine-grained intergrowths of multiple species, which makes their characterization and study especially challenging.

Haacke and Williams [69] reported the solubility of zippeites ($M_2(UO_2)_6(SO_4)_3(OH)_{10}(H_2O)_n$) with M = Mg, Co, Ni, and Zn. Pre-experimental characterization of the mineral phases involved XRD and TGA analyses. Reaching a steady state from undersaturated conditions took 2 to 3 weeks with the steady state being defined by a constant pH in the system. The authors analyzed for divalent cations with AAS and assumed stoichiometric dissolution to calculate the U and S concentrations in the system. There was no mention of any post-experimental analysis on the solid residues. When taking into account complexation of uranyl the authors did not adjust the equilibrium constants for the aqueous complexation reactions for ionic strength effects; however, the K_{sp} values were calculated using activities with activity coefficients calculated from a modified Davies equation with parameters from Truesdell and Jones [17]. The $\lg K_{sp}$ values for M = Mg, Co, Ni, and Zn are (−146.1), (−145.9), (−145.6), and (−153.0), respectively.

O'Brien and Williams [70] measured the solubility of three zippeites ($M_4(UO_2)_6(SO_4)_3(OH)_{10}(H_2O)_4$) with M = Na, K, and NH_4. The authors reference previous work [19,69] to describe their experimental procedures and calculations; therefore, it is assumed that there was no post-experimental characterization of the solid residue. Dissolution of the mineral was assumed stoichiometric based on the divalent cation analysis of the experimental solution, and K_{sp} value calculations considered ionic strength effects with a modified Davies equation with parameters from Truesdell and Jones [17], but the equilibrium constants for the aqueous complexation reactions were not adjusted for ionic strength effects. The $\lg K_{sp}$ values calculated from their reported ΔG_f° for M = Na, K, and NH_4 are (−116.5), (−116.1), and (−126.2), respectively.

Each study described above lacks rigorous constraints on the reported ΔG_f° values due to the non-validated assumption of stoichiometric dissolution, lack of post-experimental residue analysis, and absence of reversibility experiments to demonstrate achievement of equilibrium. The wide-spread nature of uranyl sulfates demonstrates the need for rigorously constrained K_{sp} values. In addition

to the phases described above, johannite ($Cu[(UO_2)_2(SO_4)_2(OH)_2](H_2O)_8$) and uranopilite ($[(UO_2)_6(SO_4)O_2(OH)_6(H_2O)_6]$) may be environmentally important.

4. Causes of variability among K_{sp} measurements

4.1. Surface free energies and particle size

For most of the uranyl minerals for which solubility data exist, there is considerable variation in the measured solubilities and calculated K_{sp} values from one study to the next. Predicting the solubility of uranyl phases under conditions not directly studied in the laboratory is one of the applications that utilize the thermodynamic data from these solubility studies. The example of becquerelite illustrates how the relatively high uncertainties associated with measured K_{sp} values lead to a large uncertainty associated with predicted mineral solubilities. Figure 2 depicts predictions of the solubility of becquerelite as a function of pH based on the results from solubility measurements using synthetic phases ($\lg K_{sp}$ values of 41.2 and 43.7) compared to the predictions based on the K_{sp} value calculated from the experiments that involved a natural becquerelite sample. The two values from the synthetic becquerelite experiments yield an order of magnitude difference in calculated U molalities at a given pH, and the K_{sp} from the natural sample experiments yields calculated U concentrations that are two to three orders of magnitude below the others. Clearly, the K_{sp} of becquerelite must be better constrained in order to reasonably estimate the mobility and distribution of U in becquerelite-buffered geologic systems. A similar degree of uncertainty in calculated U concentrations exists for a number of the other uranyl phases described here, such as uranophane and rutherfordine, and there are an even larger number of uranyl phases for which no thermodynamic data exist at all. The error associated with rigorously constrained data, such as Ilton *et al.* [47] and Gorman-Lewis *et al.* [13], gives a better indication of what degree of uncertainty can be achieved for solubility measurements.

The variation in calculated K_{sp} values for a particular uranyl phase could stem from a number of sources other than experimental error. One such source could be the influence of particle size on solubility. The particle size of microcrystalline powders with a surface area greater than a few $m^2 \cdot g^{-1}$ (that is, individual particle sizes smaller than approximately 1 μm) can substantially affect measured solubilities [71,72]. Previous research on uranyl minerals has qualitatively documented this effect [22,31,73,74]. The interfacial free energy of mineral phases is related to the particle size as shown in equation (5) [72], where $K_{sp(s)}$ is the K_{sp} of the small particle size sample, $K_{sp(s=\infty)}$ is the K_{sp} of a highly crystalline larger particle sample, $\bar{\gamma}$ is the interfacial free energy of the mineral phase, and s is the molar surface area:

$$\lg k_{sp(s)} = \lg K_{sp(s=\infty)} + \frac{\frac{2}{3}\bar{\gamma}}{RT^s}. \quad (6)$$

Lowering of the interfacial free energy of a mineral phase, through smaller particle size, increases the solubility of the phase. Different synthetic methods for growing the same mineral may produce solids with markedly different particle sizes and/or crystallinities, hence yielding significantly different solubilities. In addition, it is often necessary to repeat the same synthesis procedure multiple times in order to produce enough material for solubility experiments. The particle size of each batch of synthetic material may vary. Thus, solubility measurements of the same mineral produced from different synthetic batches may also introduce variability in solubility measurements. Measurements and reporting of the surface area of the material used in uranyl phase solubility experiments may be necessary to

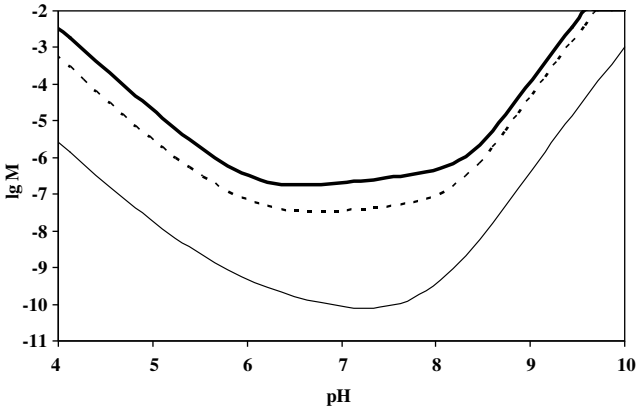

FIGURE 2. Plot of logarithm of total U in solution against pH calculated from becquerelite solubility in the presence of 10 mM Ca^{2+} and $pCO_2 = 32$ Pa with $\lg K_{sp}$ values of 29 (thin curve), 41.2 (dashed curve), and 43.7 (thick curve). The predicted solubility takes into account reactions listed in Table 2 with the exception of calcium uranyl carbonate ternary complexes.

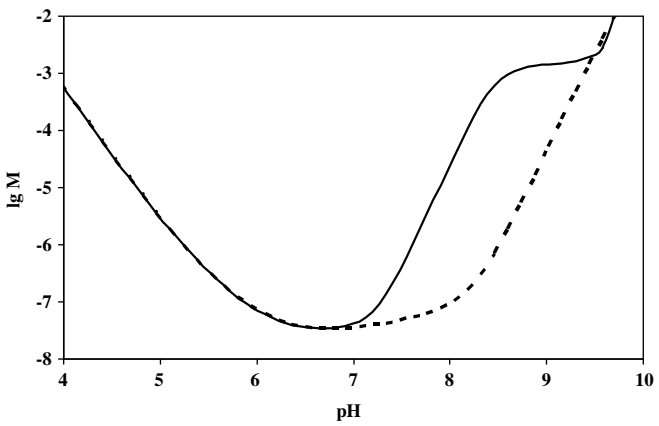

FIGURE 3. Plot of logarithm of total U in solution against pH from the predicted solubility of becquerelite with 10 mM Ca^{2+} and $pCO_2 = 32$ Pa in the presence (solid curve) and absence (dashed curve) of calcium uranyl carbonate ternary complexes. The predicted solubility takes into account reactions listed in Table 2.

account for this effect and in turn to produce more consistent solubility measurements and K_{sp} values.

4.2. Aqueous complexation reactions

Calculated values of uranyl mineral K_{sp} values are highly dependent on the thermodynamic stability constants that are used in the calculations for aqueous uranyl complexes. Below approximately pH 4 at low U concentrations (below *ca.* 10 mM), aqueous U speciation is dominated by the un-complexed uranyl species (UO_2^{+2}). Therefore, for solubility experiments conducted below pH 4 without high concentration of U in solution, one can safely assume that the measured concentration of U in solution is equivalent to the concentration of the uranyl cation. However, above approximately pH 4, aqueous uranyl hydroxide, uranyl carbonato, and mixed uranyl hydroxide-carbonato complexes become more important than the uncomplexed uranyl cation, and must be accounted for in calculations of K_{sp} values for experiments conducted under these pH conditions. Different studies have used different choices of aqueous complexation reactions to account for U speciation, and have used different values for the equilibrium constants for those reactions, so comparison of K_{sp} values from these studies is meaningless. Grenthe *et al.* [11] compiled a critically reviewed thermodynamic database of aqueous U complexation reactions and their stability constants. A number of stability constants for hydrolyzed uranyl species were estimated due to the lack of reliable data. Often, under the conditions used in solubility experiments, these hydrolyzed species are negligible and the error associated with using the estimated stability constants for these species does not affect calculated K_{sp} values. Guillaumont *et al.* [12] updated the Grenthe review and revised many of the uranyl hydroxide and uranyl carbonate stability constants by assessing new data on the thermodynamic stabilities of these complexes. These revised stability constants are, for the most part, within the error reported for the stability constants reported in Grenthe *et al.*, and are unlikely to significantly change calculated K_{sp} values. However, neither of these critical reviews included ternary complexes in their recommended list of stability constants. These ternary complexes involve the uranyl cation, the carbonate anion, and an alkaline earth metal, such as the calcium–uranyl–carbonate complex reported by Dong and Brooks [75], Bernhard *et al.* [76], and Kelly *et al.* [77] which can dominate the aqueous uranyl budget under relatively high pH conditions. The accuracy of calculations of K_{sp} values from experiments conducted under conditions favorable to the formation of this type of ternary complex depends on inclusion of these ternary complexation reactions in models of the U speciation.

The presence of these aqueous ternary complexes can dramatically affect extrapolations of uranyl mineral solubilities from the low pH conditions, under which the solubilities were measured, to circumneutral pH conditions in equilibrium with atmospheric carbon dioxide. Figure 3 illustrates the solubility of becquerelite (using the K_{sp} from Rai *et al.* [35]) in the presence and absence of aqueous calcium–uranyl–carbonate ternary complexes identified by Dong and Brooks [75]. The difference in the solubility curves is dramatic. The $CaUO_2(CO_3)_3^{2-}$ species dominates solution from *ca.* pH 7 to 9; it is this species that causes the dramatic increase in becquerelite solubility. For example, at pH 8, the presence of $CaUO_2(CO_3)_3^{2-}$ increases the solubility of becquerelite approximately two orders of magnitude, and the magnitude of the increase would be greater for solutions in which the concentration of Ca is externally buffered to higher levels.

5. Theoretical predictions

In the absence of an extensive thermodynamic database for uranyl minerals, a number of investigators have developed methods to estimate Gibbs free energies of formation for environmentally-relevant phases. One method, developed by Chen [78], considers the chemical components of a mineral phase, and assumes that the total standard state Gibbs free energy of formation of the phase is equivalent to the sum of the energies of formation of the component compounds that form the mineral. Hemingway [79] applied the Chen method to predict the Gibbs free energies of formation of a number of uranyl silicates. His predictions for soddyite, uranophane, and Na-boltwoodite differ from experimental values, determined for soddyite by Gorman-Lewis *et al.* [13], and determined for uranophane and sodium boltwoodite by Nguyen *et al.* [45], by (−33), (−2), and (46) kJ/mol, respectively. The predictions for soddyite and Na-boltwoodite are far outside the reported uncertainties associated with the experimental values; however, the uranophane prediction is within the error reported for the experimental value.

Tardy and Garrels [80] developed a linear free energy prediction approach that uses the linear relationship between the standard state Gibbs free energy of formation from the elements of a silicate and a parameter, ΔO^{2-}, defined as the difference between the Gibbs free energy of formation of oxide components found in the mineral phase and its aqueous constituents. Van Genderen and Van Der Weijden [81] used the method developed by Tardy and Garrels to predict the standard state Gibbs free energies of formation of a number of uranyl phases. Their treatment was only applicable to mineral groups with the same structure as the empirical relationship between ΔO^{2-} and the Gibbs free energy of formation of the constituent oxides, as the approach is sensitive to differences in mineral structure.

Finch [82] and Clark *et al.* [83] used a method based on the Tardy and Garrels method where the Gibbs free energy of formation of a uranyl phase is predicted by the sum of the oxide constituents. The problems associated with this technique involved the assumption that the Gibbs free energies of formation for the metal oxides that make up the mineral of interest, *e.g.* SiO_2 and Na_2O for Na-bolt-

woodite, are equal to the Gibbs free energies of formation for silicate structures in non-uranyl mineral phases. In addition, uranyl in structures can be coordinated by four, five, or six oxygen atoms in an approximately coplanar arrangement [25,84]. This method cannot account for these differences in uranyl coordination; consequently, there is systematic disagreement between the predicted and measured Gibbs free energies of formation of uranyl phases that involve coordinations not included in the calibration of the relationship.

The most recent attempt to model standard state Gibbs free energies of formation for uranyl minerals relies not on constituent oxides, but rather on sums of the contributions of constituent polyhedra or "cation oxides" [85]. Multiple regressions of the thermodynamic data for which crystal structures are known are used to determine the molar structural components. This technique attempts to afford more flexibility for predictions of phases that do not have representative phases for which thermodynamic data are available because the cation polyhedron is considered to have well defined properties. This predictive approach provides better agreement with experimental results than previous predictions. For example, the predictions by Chen *et al.* for soddyite and Na-boltwoodite ((-3653.0 ± 2.9) and (-2844.8 ± 3.9) kJ/mol, respectively) are in close agreement with values calculated from solubility measurements of soddyite by Gorman-Lewis *et al.* ((-3652.2 ± 4.6) kJ/mol) and for sodium boltwoodite by Ilton *et al.* ((-2845.2 ± 1.5) kJ/mol).

6. Conclusions

The importance of a comprehensive database of thermodynamic properties of uranyl minerals is vital for understanding the mobility of U in the environment. Presently, much of the available solubility measurements lack rigorous demonstration of the attainment of equilibrium. In addition, in many cases the experimental solid residue was not characterized to determine if the uranyl phase of interest was stable under the experimental conditions. The large variation in calculated K_{sp} values for the same mineral illustrates the uncertainty associated with the presently available data for most phases that have been studied. More rigorous measurements with proper post-experimental residue characterization, demonstration of steady state from undersaturation and supersaturation, and proper calculation of activity coefficients are essential for construction of an internally-consistent database. Equally important to better constraining the K_{sp} values for the minerals that have been studied is to expand these studies to the even larger number of potentially relevant uranyl phases that have not received attention to date. Only with accurate and internally-consistent thermodynamic data for all of the environmentally-relevant uranyl phases can we model the paragenesis associated with spent nuclear fuel alteration. A comprehensive database is required to model not only the relative stabilities of various uranyl minerals as a function of geologic conditions, but also to predict the concentration of U and other elements in equilibrium with these dominant uranyl phases under a range of conditions not directly studied in the laboratory.

Acknowledgements

Funding for this research was provided by a US Department of Energy, Office of Science and Technology and International (OST&I) Grant under the Source Term Thrust program. Two journal reviews significantly improved the presentation of the manuscript.

References

[1] R.J. Finch, R.C. Ewing, J. Nucl. Mater. 190 (1992) 133–156.
[2] R.J. Finch, E.C. Buck, P.A. Finn, J.K. Bates, Mater. Res. Soc. Symp. Proc. 556 (1999) 431–438.
[3] D.J. Wronkiewicz, J.K. Bates, T.J. Gerding, E. Veleckis, B.S. Tani, J. Nucl. Mater. 190 (1992) 107–127.
[4] D.J. Wronkiewicz, J.K. Bates, S.F. Wolf, E.C. Buck, J. Nucl. Mater. 238 (1996) 78–95.
[5] T. Murakami, T. Ohnuki, H. Isobe, T. Sato, Am. Mineral. 82 (1997) 888–899.
[6] E.C. Pearcy, J.D. Prikryl, W.M. Murphy, B.W. Leslie, Appl. Geochem. 9 (1994) 713–732.
[7] J.G. Catalano, S.M. Heald, J.M. Zachara, G.E. Brown, Environ. Sci. Technol. 38 (2004) 2822–2828.
[8] Y. Roh, S.R. Lee, S.K. Choi, M.P. Elless, S.Y. Lee, Soil Sediment. Contam. 9 (2000) 463–486.
[9] J.B. Gillow, M. Dunn, A.J. Francis, D.A. Lucero, H.W. Papenguth, Radiochim. Acta 88 (2000) 769–774.
[10] A.J. Francis, C.J. Dodge, J.B. Gillow, H.W. Papenguth, Environ. Sci. Technol. 34 (2000) 2311–2317.
[11] I. Grenthe, J. Fuger, R.J. Konings, R.J. Lemire, A.B. Muler, C. Nguyen-Trung, H. Wanner, Chemical Thermodynamics of Uranium, Elsevier, Amsterdam, 1992.
[12] R. Guillaumont, T. Fanghanel, J. Fuger, I. Grenthe, V. Neck, D. Palmer, M. Rand, Update on the Chemical Thermodynamics of Uranium, Neptunium, and Plutonium, second ed., Elsevier, Amsterdam, 2003.
[13] D.J. Gorman-Lewis, L. Mazeina, B. Fein Jeremy, J. Szymanowski, P.C. Burns, A. Navrotsky, J. Chem. Thermodyn. 39 (2007) 568–575.
[14] H.C. Helgeson, D.H. Kirkham, G.C. Flowers, Am. J. Sci. 281 (1981) 1249–1516.
[15] D.L. Clark, D.E. Hobart, M.P. Neu, Chem. Rev. 95 (1995) 25–48.
[16] K. Alwan, P.A. Williams, Mineral. Mag. 43 (1980) 665–667.
[17] A.H. Truesdell, B.F. Jones, J. Res. US Geol. Surv. 2 (1974) 238.
[18] J. Kielland, J. Am. Chem. Soc. 59 (1937) 1675.
[19] T.J. O'Brien, P.A. Williams, Mineral. Mag. 47 (1983) 69–73.
[20] H.R. Westrich, W.H. Casey, G.W. Arnold, Geochim. Cosmochim. Acta 53 (1989) 1681–1685.
[21] G. Meinrath, T. Kimura, Inorg. Chim. Acta 204 (1993) 79–85.
[22] G. Meinrath, Y. Kato, T. Kimura, Z. Yoshida, Radiochim. Acta 75 (1996) 159–167.
[23] U. Kramer-Schnabel, H. Bischoff, R.H. Xi, G. Marx, Radiochim. Acta 56 (1992) 183–188.
[24] P.C. Burns, Y. Li, Am. Mineral. 87 (2002) 550–557.
[25] P.C. Burns, P.C. Ewing, M.L. Miller, J. Nucl. Mater. 245 (1997) 1–9.
[26] P.C. Burns, K.M. Deely, S. Skanthakumar, Radiochim. Acta 92 (2004) 151–159.
[27] M. Douglas, S.B. Clark, J.I. Friese, B.W. Arey, E.C. Buck, B.D. Hanson, Environ. Sci. Technol. 39 (2005) 4117–4124.
[28] P.C. Burns, A.L. Klingensmith, Elements 2 (2006) 351–356.

[29] A.G. Sowder, S.B. Clark, R.A. Field, Environ. Sci. Technol. 33 (1999) 3552–3557.
[30] R.J. Finch, F.C. Hawthorne, R.C. Ewing, Can. Mineral. 36 (1998) 831–845.
[31] A. Sandino, J. Bruno, Geochim. Cosmochim. Acta 56 (1992) 4135–4145.
[32] D.E. Giammar, J.G. Hering, Environ. Sci. Technol. 38 (2004) 171–179.
[33] J. Bruno, A. Sandino, Mater. Res. Soc. Symp. Proc. 127 (1989) 871–878.
[34] P.D. Arocas, B. Grambow, Geochim. Cosmochim. Acta 62 (1998) 245–263.
[35] B.D. Rai, A.R. Felmy, N.J. Hess, V.L. LeGore, D.E. McCready, Radiochim. Acta 90 (2002) 495–503.
[36] I. Casas, J. Bruno, E. Cera, R.J. Finch, R.C. Ewing, Geochim. Cosmochim. Acta 61 (1997) 3879–3884.
[37] J.V. Walther, H.C. Helgeson, Am. J. Sci. 277 (1977) 1315–1351.
[38] M.C.A. Sandino, B. Grambow, Radiochim. Acta 66–67 (1994) 37–43.
[39] R. Vochten, L. Van Haverbeke, Miner. Petrol. 43 (1990) 65–72.
[40] M. Atkins, A.N. Beckley, F.P. Glasser, Radiochim. Acta 44–45 (1988) 255–261.
[41] R. Finch, T. Murakami, Rev. Mineral. Geochem. 38 (1999) 91–179.
[42] P.C. Burns, Can. Mineral. 36 (1998) 1069–1075.
[43] P.A. Finn, J.C. Hoh, S.F. Wolf, S.A. Slater, J.K. Bates, Radiochim. Acta 74 (1996) 65–71.
[44] D.E. Giammar, J.G. Hering, Geochim. Cosmochim. Acta 66 (2002) 3235–3245.
[45] S.N. Nguyen, R.J. Silva, H.C. Weed, J.E. Andrews, J. Chem. Thermodyn. 24 (1992) 359–376.
[46] P.C. Burns, in: P.C. Burns, R.J. Finch (Eds.), The Crystal Chemistry of Uranium, Mineralogical Society of America, Washington, DC, 1999, pp. 23–90.
[47] E.S. Ilton, C.X. Liu, W. Yantasee, Z.M. Wang, D.A. Moore, A.R. Felmy, J.M. Zachara, Geochim. Cosmochim. Acta 70 (2006) 4836–4849.
[48] I. Casas, J. Bruno, E. Cera, R.J. Finch, R.C. Ewing, Kinetic and thermodynamic studies of uranium minerals assessment of the long-term evolution of spent nuclear fuel, Swedish Nuclear Fuel and Waste Management Co., SKB Technical Report 94-16. Stockholm, Sweden, 1994.
[49] I. Perez, I. Casas, M. Martin, J. Bruno, Geochim. Cosmochim. Acta 64 (2000) 603–608.
[50] H. Moll, G. Geipel, W. Matz, G. Bernhard, H. Nitche, Radiochim. Acta 74 (1996) 3–7.
[51] E.C. Buck, N.R. Brown, N.L. Dietz, Environ. Sci. Technol. 30 (1996) 81–88.
[52] L.E. Macaskie, K.M. Bonthrone, P. Yong, D.T. Goddard, Microbiol.–UK 146 (2000) 1855–1867.
[53] G. Basnakova, A.J. Spencer, E. Palsgard, G.W. Grime, L.E. Macaskie, Environ. Sci. Technol. 32 (1998) 760–765.
[54] C.C. Fuller, J.R. Bargar, Abstr. Pap. Am. Chem. Soc. 222 (2001) U491.
[55] C.C. Fuller, J.R. Bargar, J.A. Davis, M.J. Piana, Environ. Sci. Technol. 36 (2002) 158–165.
[56] V. Vesely, V. Pekarek, M. Abbrent, J. Inorg. Nucl. Chem. 27 (1965) 1159–1166.
[57] M. Markovic, N. Pavkovic, Inorg. Chem. 22 (1983) 978–982.
[58] M. Markovic, N. Pavkovic, N.D. Pavkovic, J. Res. Nat. Bur. Stand. 93 (1988) 557–563.
[59] D. Rai, Y.X. Xia, L.F. Rao, N.J. Hess, A.R. Felmy, D.A. Moore, D.E. McCready, J. Solution Chem. 34 (2005) 469–498.
[60] N. Pavkovic, M. Markovic, B. Kojicprodic, Croat. Chem. Acta 55 (1982) 393–403.
[61] L. VanHaverbeke, R. Vochten, K. VanSpringel, Mineral. Mag. 60 (1996) 759–766.
[62] K.A.H. Kubatko, K.B. Helean, A. Navrotsky, P.C. Burns, Science 302 (2003) 1191–1193.
[63] B. McNamara, B. Hanson, E. Buck, C. Soderquist, Radiochim. Acta 93 (2005) 169–175.
[64] G. Sattonnay, C. Ardois, C. Corbel, J.F. Lucchini, M.F. Barthe, F. Garrido, D. Gosset, J. Nucl. Mater. 288 (2001) 11–19.
[65] B.E. Burakov, E.E. Strykanova, E.B. Anderson, Mater. Res. Soc. Symp. Proc. 465 (1997) 1309.
[66] R. Djogic, V. Cuculic, M. Branica, Croat. Chem. Acta 78 (2005) 575–580.
[67] C. Frondel, US Geol. Surv. Bull. (1958) 1064.
[68] J. Brugger, P.C. Burns, N. Meisser, Am. Mineral. 88 (2003) 676–685.
[69] D.F. Haacke, P.A. Williams, Mineral. Mag. 43 (1979) 539–541.
[70] T.J. Obrien, P.A. Williams, Inorg. Nucl. Chem. Lett. 17 (1981) 105–107.
[71] C.I. Steefel, P. Vancappellen, Geochim. Cosmochim. Acta 54 (1990) 2657–2677.
[72] W. Stumm, J.J. Morgan, Aquatic Chemistry: Chemical Equilibria and Rates in Natural Waters, third ed., Wiley, John & Sons, 1995.
[73] T. Fanghanel, V. Neck, Pure Appl. Chem. 74 (2002) 1895–1907.
[74] M.E. Torrero, I. Casas, J. Depablo, M.C.A. Sandino, B. Grambow, Radiochim. Acta 66–67 (1994) 29–35.
[75] W.M. Dong, S.C. Brooks, Environ. Sci. Technol. 40 (2006) 4689–4695.
[76] G. Bernhard, G. Geipel, T. Reich, V. Brendler, S. Amayri, H. Nitsche, Radiochim. Acta 89 (2001) 511–518.
[77] S.D. Kelly, K.M. Kemner, S.C. Brooks, Geochim. Cosmochim. Acta 71 (2007) 821–834.
[78] C.H. Chen, Am. J. Sci. 275 (1975) 801–817.
[79] B.S. Hemingway, Thermodynamic properties of selected uranium compounds at 298.15 K and 1 bar and at higher temperatures – preliminary models for the origin of coffinite deposits, Open-File, 82-619, USGS Open-File Report 82-619, 1982.
[80] Y. Tardy, R.M. Garrels, Geochim. Cosmochim. Acta 41 (1977) 87–92.
[81] L.C.G. Van Genderen, C.H. Van Der Weijden, Uranium 1 (1984) 249–256.
[82] R.J. Finch, Mater. Res. Soc. Symp. Proc. 465 (1997) 1185–1192.
[83] S.B. Clark, R.C. Ewing, J.C. Schaumloffel, J. Alloys Compd. 271 (1998) 189–193.
[84] P.C. Burns, M.L. Miller, R.C. Ewing, Can. Mineral. 34 (1996) 845–880.
[85] F.R. Chen, R.C. Ewing, S.B. Clark, Am. Mineral. 84 (1999) 650–664.
[86] A.E. Martell, in: NIST Critically Selected Stability Constants of Metal Complexes, Gaithersburg, MD, 2001.

JCT 07-300